Wrist Anatomy

2

2.1 Ligaments of the Wrist and their Functional Significance

2.1.1 Overview of Carpal Ligament Organization

The ligaments of the wrist can be categorized by generic divisions (intrinsic vs. extrinsic), by location (palmar versus dorsal, radiocarpal versus midcarpal), or by function (guiding, constraining) [1]. The differentiation of the wrist ligaments into intrinsic (intra-articular or interosseous) and extrinsic (capsular) is based on histological criteria. Moreover, the intrinsic ligaments originate and insert on the carpal bones, while extrinsic ligaments course between the carpal bones and the radius or the metacarpals [2]. Both intrinsic and extrinsic ligaments consist of relatively parallel groups of densely packed, highly organized collagen fibers called *fascicles*. The fascicles are surrounded by regions of poorly organized connective tissue, called *perifascicular* spaces. Near the periphery of the ligament, the perifascicular spaces coalesce to form the *epiligamentous sheath*. The superficial surface of a capsular ligament forms the *fibrous stratum* of the epiligamentous sheath, while on the deep, or joint surface of the ligament, the epiligamentous sheath forms a continuous layer called the *synovial stratum* of the epiligamentous sheath. Intrinsic (intra-articular) ligaments are covered entirely by a synovial stratum, whereas extrinsic (capsular) ligaments have the synovial stratum only on their deep or joint surface [1].

A third category of ligaments has been described [1, 3] by the term *meniscocapsular* ligaments referring to a synovial capsular structure containing massive concentrations of blood vessels and nerves. A typical example of such a structure is the radioscapholunate ligament (RSL).

There is some degree of function overlap between the intrinsic and extrinsic ligaments leading to a temporary counterbalance after an individual ligament injury. That equilibrium may be exceeded with cyclic loading following an injury and this progressively leads to insufficiency of the secondary ligamentous constraints and an initially normal radiographic image becomes over time diagnostic of the instability. A typical example of this progressively evolving instability is the scapholunate and lunotriquetral dissociation. Berger in 1997 [4] prophetically argued what was in recent years confirmed: “We tend to look upon the carpal ligaments as passive bands of collagen constraining the action of the bones that they connect. The rich innervation of the ligaments, however, may introduce an entirely new consideration of function for the ligaments as end organs of mechanoreception. It is possible that the wrist is stabilized by a mixture of static structures such as ligaments and dynamic structures such as muscles. As such, the ligaments may play roles as both static support and sensory organs”.

E. Apergis, *Fracture-Dislocations of the Wrist*,
DOI: 10.1007/978-88-470-5328-1_2, © Springer-Verlag Italia 2013

Table 2.1 The ligaments of the wrist and their acronyms used in the book

Extrinsic or capsular ligaments		
Radiocarpal (RC) joint	Palmar	Radioscaphocapitate (RSC)
		Long radiolunate (LRL)
		Short radiolunate (SRL)
		Radioscapholunate (RSL)
	Dorsal	Dorsal radiocarpal (Dorsal RC)
Midcarpal (MC) Joint	Palmar	Scapho-trapezium-trapezoid (STT)
		Scaphocapitate (SC)
		Capitate trapezium (CTm)
		Triquetrocapitate (TC)
		Triquetrohamate (TH)
		Palmar scaphotriquetral (Palmar ST)
	Dorsal	Dorsal intercarpal (DIC)
		Dorsal scaphotriquetral (Dorsal ST)
Ulnocarpal (UC) joint		Ulnolunate (UL)
		Ulnotriquetral (UT)
		Ulnocapitate (UC)
Distal radioulnar joint (DRUJ)		Triangular fibrocartilage complex (TFCC)
		Dorsal radioulnar (DRU)
		Palmar radioulnar (PRU)
		Meniscus homologue (MH)
Intrinsic or intra-articular or interosseous ligaments		
Proximal carpal row		Scapholunate interosseous (SLI)
		Lunotriquetral interosseous (LTI)
Distal carpal row		Trapeziotrapezoid (TT)
		Trapeziocapitate (TC)
		Capitohamate (CH)

To date, the detailed carpal ligament nomenclature and classification by Berger is the most commonly cited and most detailed of all [5], therefore this is mainly used in this book.

Table 2.1 shows aggregately all the wrist ligaments and the acronyms described in this book.

2.1.2 Extrinsic or Capsular Ligaments: Volar Surface

2.1.2.1 Radiocarpal Joint

The palmar radiocarpal ligaments originate from the palmar rim of the distal radius, attaching approximately 1–2 mm proximal to the articular surface and coursing distally, attach to one or more carpal bones (Figs. 2.1 and 2.2). These ligaments constitute the main stabilizing structures of the radiocarpal joint and are best viewed from an intra-articular perspective.

Radioscaphocapitate ligament (RSC ligament)

The RSC ligament is the most radial of the palmar radiocarpal ligaments that originates proximally from a roughened area on the palmar and radial aspects of the radial styloid process [4]. It courses distally and ulnarly and attaches partially to the radial surface of the waist of the scaphoid and to the proximal cortex of the distal scaphoid pole

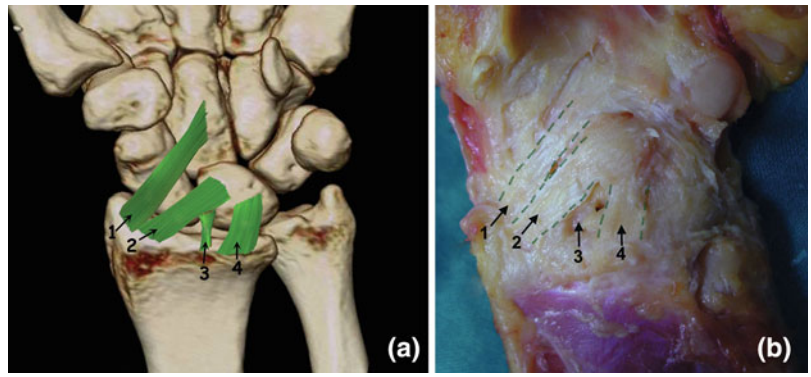

Fig. 2.1 Schematic (**a**) and cadaveric (**b**) depiction of palmar radiocarpal ligaments: radioscaphocapitate (*1*), long radiolunate (*2*), radioscapholunate (Testut) (*3*), short radiolunate (*4*)

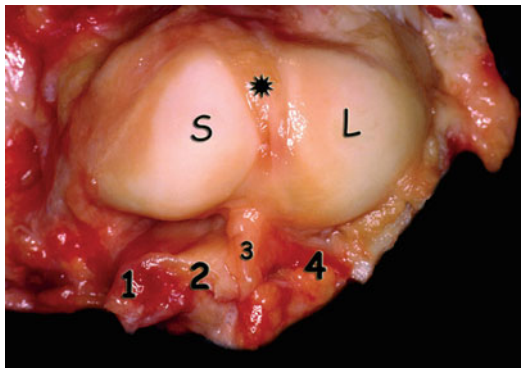

Fig. 2.2 Palmar radiocarpal ligaments: Radioscaphocapitate (*1*), Long radiolunate (*2*), Radioscapholunate (Testut) (*3*), short radiolunate (*4*). The *asterisk* indicates scapholunate ligaments. Scaphoid (*S*), lunate (*L*). With permission from [157]

together with the palmar scaphotriquetral ligament (Palmar ST ligament) [6, 7]. The majority of its fibers pass anterior to the waist of the scaphoid to form the palmar capsule of the midcarpal joint. The percentage of fibers that attach to the capitate neck varies. Berger [1, 4] estimated that only 10 % of its fibers actually insert into the palmar cortex of the capitate. The remaining fibers course ulnarly interdigitating with fibers from the ulnocapitate and triquetrocapitate ligaments to form the *arcuate (deltoid or V) ligament* [4, 8]. In contrast to these findings, Buijze et al. [5, 6] found that the bulk of fibers seem to insert mostly on the capitate and do not seem to interdigitate predominantly with fibers arching toward the ulna and triquetrum.

The RSC is separated from the LRL ligament by a deep division called the interligamentous sulcus, which is more obvious intraarticularly. This sulcus, between lunate and capitate, constitutes a weak area of the joint capsule known as *space of Poirier*. The RSC ligament is approximately 1.4 mm thick, 29.8 mm long, and 5.1 mm wide [6].

A number of functions have been attributed to this ligament: (a) Some of its fibers form a radial collateral ligament [9], which is a controversial ligament as its existence is disputed. The greatest controversy is whether it is a separate ligament or the most radial bundle of the RSC ligament, (b) provides resistance to passive pronation of the radiocarpal joint [10], (c) along with the other palmar radiocarpal ligaments provides restraint to dorsal translation of the carpus [11], (d) constrains ulnar translation of the carpus [4, 12, 13], (e) stabilizes the distal pole of the scaphoid [4, 10], and (f) acts as a fulcrum around which the scaphoid rotates [14].

The force required for rupture of the radial collateral region is approximately 100 N, compared with approximately 150 N for rupture of the radiocapitate region. Strain rates at rupture average approximately 125 % and 75 %, respectively [4, 15].

Styloidectomy, depending on the size and morphology, affects in different degrees the origin of the palmar radiocarpal ligaments [16]. Great care must be taken to avoid damage to this ligament in cases of scaphoid excision (proximal row carpectomies, SLAC wrists) [17, 18].

Long Radiolunate Ligament (LRL ligament) (Palmar Radiolunotriquetral Lig., Palmar Radiotriquetral Lig.)

The LRL is a large capsular ligament that originates proximally from the palmar rim of the scaphoid fossa of the distal radius, just ulnar to the RSC ligament. The length, width, and thickness of the LRL are approximately 16, 5.8, and 1.2 mm, respectively [19]. The proximal attachment of the LRL is partially overlapped by the radioscaphocapitate ligament [20, 21] (Fig. 2.3). It courses obliquely distally and ulnarly anterior to the proximal pole of the scaphoid and anterior to the SL joint, overlapping completely the volar scapholunate interosseous ligament (SLI Ligament), to insert widely on the palmar horn of the lunate [3]. The degree of attachment to the lunate may vary between individuals. Some authors [7, 22] have suggested that this ligament continues ulnarly inserting to the palmar surface of the triquetrum, between the insertion of the palmar ulnotriquetral ligament (UT ligament) proximally and the insertion of the Palmar ST ligament distally, forming the radiolunotriquetral ligament. It has been supported that only the fibrous stratum of the joint capsule continues toward the triquetrum and not the fibers of the ligament, thus the designations of the radiolunotriquetral and radiotriquetral ligaments are misleading [3, 4].

Functions attributed to this ligament are: (a) along with the short radiolunate, it functions as a primary restraint to ulnar translocation of the lunate [4, 23], (b) participates in the formation of the antipronation sling, which is responsible for the control of intracarpal pronation [10, 24].

Material property testing of the LRL ligament shows that it ruptures at approximately 110 N of applied force, with approximately 125 % strain at rupture [15].

Radioscapholunate ligament (RSL ligament) (Testut or Testut and Kuenz Ligament)

It is located between the LRL and short radiolunate ligament (SRL) ligaments, originating from the prominence between the scaphoid and lunate articular facets on the distal articular surface of the radius (Figs. 2.1, 2.2, and 2.3).

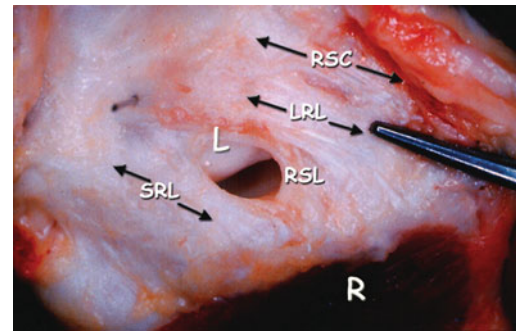

Fig. 2.3 Palmar radiocarpal ligaments: radioscaphocapitate (*RSC*), long radiolunate (*LRL*), radioscapholunate (*RSL*), short radiolunate (*SRL*). *R* radius. With permission from [157]

Vertically oriented, it perforates the palmar joint capsule inserting into the proximal and palmar aspects of the scapholunate ligament [20, 25, 26]. It is approximately 0.7–1.2 mm thick, 8.3–9 mm long, and 2.5–4.8 mm wide [6, 20]. Its arthroscopic appearance is characterized as intra-articular fat pad [27, 28].

Various studies showed that this ligament presents a number of particularities:

(a) The RSL is morphologically distinguished from the other palmar radiocarpal ligaments by its loosely organized collagen fibers and relatively high degree of vascularity [25]. The vessels originate from the radial carpal arch, which is an anastomotic vessel between the anterior interosseous and radial arteries while the nerve fibers are terminal branches of the anterior interosseous nerve [4]. It is probably not a true ligament but a neurovascular conduit to the SLI Ligament with little mechanical integrity [29].

(b) The ligament possibly constitutes a fetal remnant of a septum that temporarily divides the radiocarpal joint into radioscaphoid and radiolunate clefts [4].

(c) Biomechanical studies showed that it is a rather weak ligament failing at approximately 40 N of applied load, but with substantial elastic behavior and higher strain at failure—approximately 175 % [15].

(d) Although its mechanical contribution is disputed, it may be important to the functional

integrity of the wrist [26]. There is increasing evidence that it plays a role as a mechanoreceptor monitoring the SL relationship, with afferents through the anterior interosseous nerve [4]. It is also a likely source for synovial filtration, producing synovial fluid and possibly resorbing metabolic waste.

Short Radiolunate Ligament (SRL ligament)

This ligament originates from the ulnopalmar edge of the distal radius and inserts at the junction of the proximal articular surface and the nonarticular palmar horn of the lunate, proximal to the insertion of the ulnolunate ligament (UL ligament) [3] (Fig. 2.4). The length, width, and thickness of the SRL are approximately 7.5, 10.6, and 1.2 mm, respectively [20]. The orientation of its fibers is changed from fan shaped in palmar flexion to longitudinal in dorsiflexion of the lunate [3, 4]. Although its functional role has not been fully clarified, it seems that it stabilizes the lunate (and hence the proximal carpal row) and prevents its volar, dorsal, and ulnar translation. The deficiency of the SRL is mainly responsible for the dorsal subluxation of the radiocarpal joint during the dorsal stress test of the wrist, (Fig. 2.5a, b) while the SRL has been considered the primary soft tissue restraint against volar translation of the carpus [9]. Consequently, fracture of the volar radial rim where the SRL ligament is attached, could destabilize the carpus leading to volar subluxation of the wrist (Fig. 2.6).

The SRL and LRL ligaments remain intact during a perilunate or lunate dislocation of the wrist, except in cases where the lunate is extirpated to the volar surface of the radius.

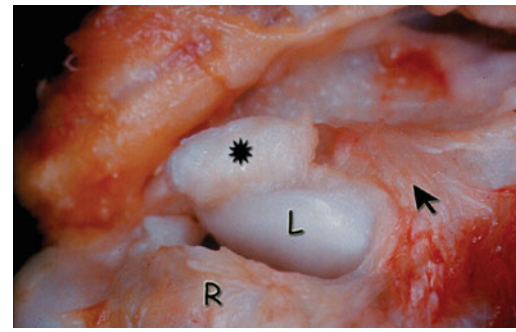

Fig. 2.4 The SRL ligament has been inverted from the volar radial rim (*asterisk*). *Arrow* indicates the LRL ligament (*R* radius, *L* lunate). With permission from [157]

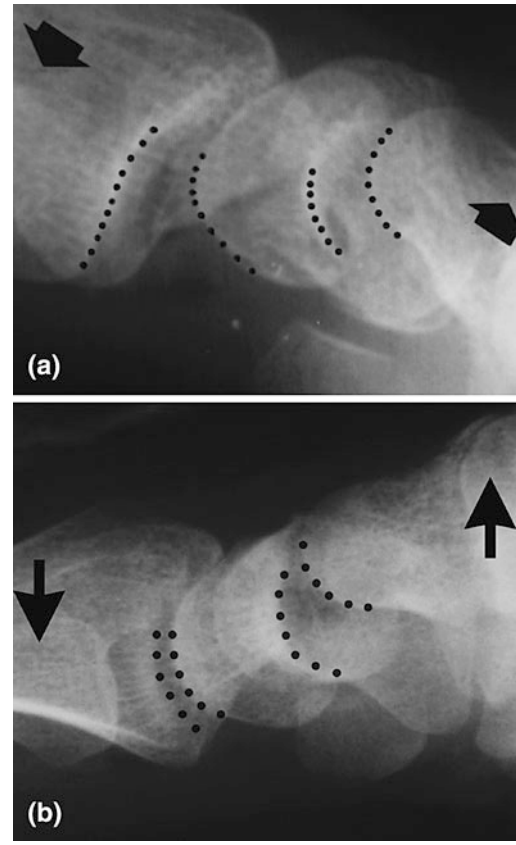

Fig. 2.5 A lax or insufficient SRL ligament could be responsible for dorsal subluxation of the radiolunate joint (**a**), while slacking of the arcuate ligament leads to subluxation of the lunocapitate joint during dorsal stress test (**b**). With permission from [157]

2.1.2.2 Ulnocarpal Joint

The ulnocarpal ligaments form the anterior and ulnar aspects of the ulnocarpal joint capsule [4]. These ligaments are responsible for maintaining the stability of the ulnocarpal joint, ensuring a correct axial alignment between the ulna and the ulnar side of the wrist [30] and also play an important role in the antero–posterior stability of the ulnar carpus [31, 32] or a significant restraint to dorso–palmar translation of the radiocarpal joint [11]. In addition, being part of the

Fig. 2.6 Fracture of the ulnovolar radial rim, where the SRL ligament attaches, could destabilize the wrist

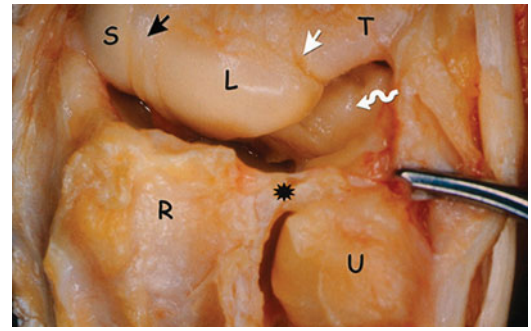

Fig. 2.8 The ulnocarpal ligaments from the dorsal side (*wavy arrow*), scapholunate ligament (*black arrow*), lunotriquetral ligament (*white arrow*), dorsal radioulnar ligament (*asterisk*) (*S* scaphoid, *L* lunate, *T* triquetrum, *R* radius, *U* ulna). With permission from [157]

ligamentous components of the TFCC, they contribute to the stability of the distal radioulnar joint (DRUJ) [23, 33] (Figs. 2.7 and 2.8).

Rupture or elongation of the ulnocarpal ligaments may lead to supination deformity of the ulnar carpus [34]. In perilunate dislocations, the infrequent finding of ruptured ulnocarpal ligaments probably indicates a reverse path of injury namely from ulnar to radial, while in cases of radiocarpal dislocations the rupture of ulnocarpal ligaments leeds to progression of the injury from ulnar translocation to multidirectional instability [35].

Ulnolunate Ligament (UL ligament)

It is located in continuity with the SRL ligament joining the formation of the volar capsule, ulnarly of the lunate fossa. It originates from the radial-most region of the volar radioulnar ligament and coursing directly distally, attaches on the volar edge of the lunate. This ligament shows similar changes in shape as the SRL ligament during dorsiflexion and palmarflexion of the wrist. The precise function of the UL ligament is not known, but it is reasonable to assume that it mirrors the function of the SRL ligament, proximally stabilizing the lunate during all phases of wrist motion [4].

Material property studies reveal that the UL ligament fails at approximately 175 N of applied load at approximately 125 % strain [15]. The length, width, and thickness of the UL ligament are approximately 18, 2.3, and 0.7 mm, respectively [20].

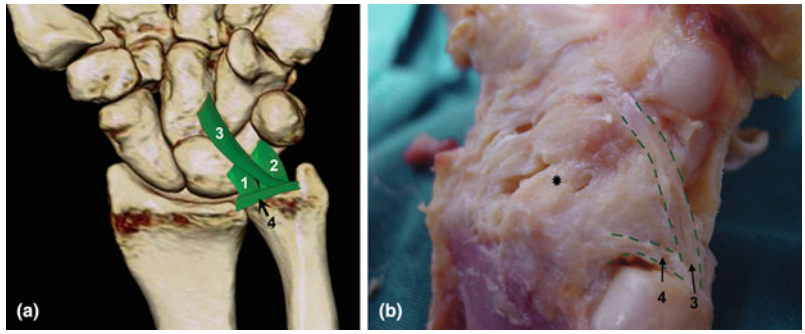

Fig. 2.7 Schematic (**a**) and cadaveric (**b**) depiction of ulnocarpal ligaments: Ulnolunate (*1*), Ulnotriquetral (*2*), Ulnocapitate (*3*), Volar radioulnar ligament (*4*) (*asterisk* short RL ligament)

Ulnotriquetral Ligament (UT ligament)

It is located ulnar to UL ligament and takes origin from the volar radioulnar ligament. It courses directly distally to insert into the proximal and palmar surface of the triquetrum. Two perforations have been found to its substance: one distally, found in more than 70 % of normal adults, leading to the pisotriquetral joint (pisotriquetral orifice) and one proximally, called the prestyloid recess that communicates with the ulnar styloid process [1] (Fig. 2.9). These two perforations constitute areas of ligamentous weakness, which can lead to longitudinal split tears of the UT ligament [36]. The medial border of the UT ligament forms the ulnar and dorsal wall of the ulnocarpal joint and the deep surface of the ECU tendon sheath as it traverses the ulnocarpal joint.

There is no clear delineation between the ulnolunate and ulnotriquetral ligaments, the division between the two being made only by their distal attachments [1].

Ulnocapitate Ligament (UC ligament)

The UC ligament is the only ulnocarpal ligament that attaches directly to the fovea region of the ulnar head. It passes distally across the ulnocarpal joint, superficial to the UT and UL ligaments. It is therefore not visible from an intra-articular perspective. Passing distally and anterior to the junction between the other ulnocarpal ligaments, at the level of lunotriquetral joint it interdigitates with fibers from the palmar region of the LT interosseous ligament. It courses around the distal margin of the palmar horn of the lunate, interdigitating with fibers from the RSC ligament, forming an "arcuate" (deltoid) ligament [4, 36]. As with the RSC ligament, only approximately 10 % of the fibers of the UC ligament actually attach to the body of the capitate [1]. Proximal to the apex of the arcuate ligament an area of weakness is located (space of Poirier), through which the midcarpal joint dislocates in perilunate injuries. The UC ligament may serve to reinforce the ulnocarpal joint capsule and the LT joint, while disruption of the UC ligament may have implications in the stability of the DRU joint [4].

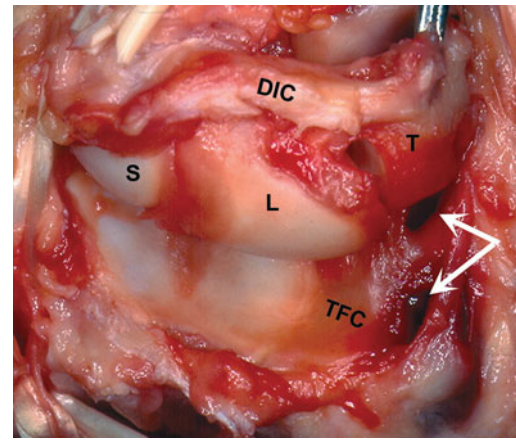

Fig. 2.9 The radiocarpal and ulnocarpal joints from the dorsal side. *White arrows* indicate the prestyloid recess (proximally) and the pisotriquetral orifice (distally). (*DIC* Dorsal intercarpal ligament, *S* scaphoid, *L* lunate, *T* triquetrum, *TFC* triangular fibrocartilage disk). In this specimen, rupture of the proximal LT ligament is evident. With permission from [157]

There has been some confusion regarding the origin of the ulnocarpal ligaments. Berger [1, 3] argued that UL and UT ligaments take origin from the volar radioulnar ligament, while the UC ligament originates directly from the fovea of the ulnar head. On the contrary, Moritomo et al. [33] stated that all ulnocarpal ligaments originate together at the fovea of the ulnar head and at the base of the ulnar styloid process. He supports that the discrepancy is due to the perspective view of the ligaments. Inspecting the ligaments arthroscopically, their origin appears to be along the volar radioulnar ligament. When inspected from the palmar side on cadavers, the ulnocarpal ligaments appear to converge into the fovea. Probably arthroscopically seeing, only part of the ligaments is visible and in fact the fibers of these ligaments extend proximally toward the fovea, although some fibers of the ligaments blend with the volar radioulnar ligament. However, it has been argued that the attachment of the ulnocarpal ligaments to the periphery of the TFC constitutes a phylogenic modification, which is necessary in order to increase the range of pronosupination without impairing the ulnocarpal joint stability [1, 30].

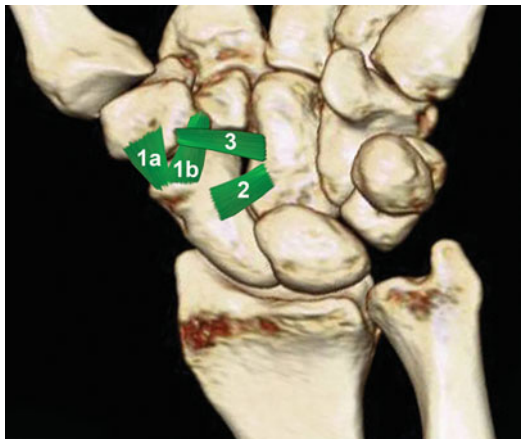

Fig. 2.10 Volar ligaments on the radial side of the midcarpal joint. Scapho-trapezium-trapezoid ligament (STT ligament) with its radial (*1a*) and ulnar band (*1b*); scaphocapitate ligament (*2*) and capitate–trapezium ligament (*3*)

2.1.2.3 Midcarpal Joint

Scapho-Trapezium-Trapezoid Ligament (STT ligament)

The STT ligament originates proximally from the radiovolar aspect of the scaphoid tuberosity, distal to the attachment of the RSC ligament. Coursing distally, it fans out to form two variably evident bands: the radial (scaphotrapezium) band forms a V-shaped structure, which attaches to the palmar and radial aspects of the trapezium. The ulnar (scaphotrapezoid) band attaches to the palmar surface of the trapezoid [1, 21, 37] (Fig. 2.10). It is the main stabilizing structure of the STT joint and is closely related to the sheath of the flexor carpi radialis tendon. Many authors [4, 38–40] studied clinically, experimentally and, biomechanically the STT ligamentous complex and made the following observations: (a) The predominant role of the distal ligamentous complex of the scaphoid over the SL ligament, which is thought to be half as strong as the distal ligamentous complex of the scaphoid, has been experimentally shown [38]. The existence of an intact STT ligament explains the absence of rotatory subluxation of the scaphoid in cases of scapholunate dissociation. (b) Scaphoid tuberosity fractures are equivalent to avulsion of the scaphotrapezial ligament [39]. (c) The axis of motion of the distal pole of the scaphoid passes through the origin of the scaphotrapezial ligament [39, 40]. (d) Although the exact function of the STT ligament remains unclear, it is believed that its principal function is to assist in maintaining the scaphoid in a palmar-flexed attitude preventing it from lying horizontally (with SL complex intact) [38], while it simultaneously minimizes excessive scaphoid flexion [39]. (e) It has been identified as an important secondary stabilizer of the scaphoid [41, 42].

Material property studies demonstrate yield strength of the STT ligament of approximately 150 N and a strain of failure at approximately 275 % [15].

Scaphocapitate Ligament (SC ligament)

The SC ligament is a strong band that obliquely crosses the palmar midcarpal joint, coursing immediately distal to the RSC ligament. It originates from the ulnar and volar side of the distal pole of the scaphoid and inserts to the radial and volar side of the capitate [4, 21] (Fig. 2.10). The SC ligament functions as a stabilizer of the distal pole of the scaphoid [4] and it may also contribute as a constraint of midcarpal pronation participating to the formation of the antipronation sling [24, 43]. A line connecting the origin of the scaphotrapezium ligament and the SC ligament is perpendicular to the interfacet ridge of the distal scaphoid, indicating that they function as collateral ligaments of a monoaxial articulation [44], and consequently, are the only ligaments guiding dart-throwing motion [45, 46]. The SC ligament is approximately 2.2 mm thick, 14 mm long, and 6.7 mm wide. It is the thickest ligament attached to the scaphoid and has the largest attachment surface area of all scaphoid ligaments [6]. Material property studies have shown average yield strength of the SC ligament of approximately 100 N and a strain of failure at approximately 200 %.

Capitate–Trapezium Ligament (CTm ligament)

The C–Tm ligament was found to originate from the radiovolar aspect of the trapezium, just under the flexor carpi radialis sheath and inserts directly

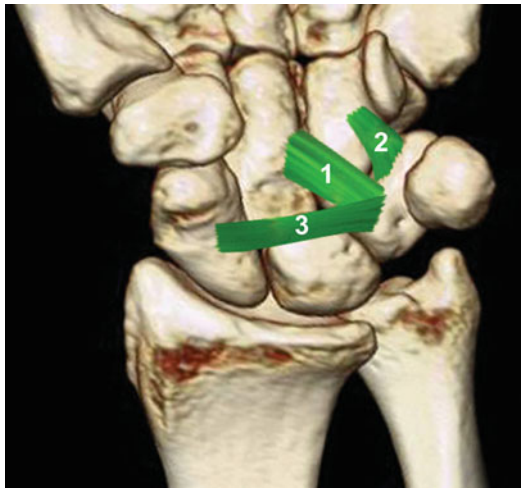

Fig. 2.11 Volar ligaments on the ulnar side of the midcarpal joint: triquetrocapitate (*1*), triquetrohamate (*2*), palmar scaphotriquetral (*3*)

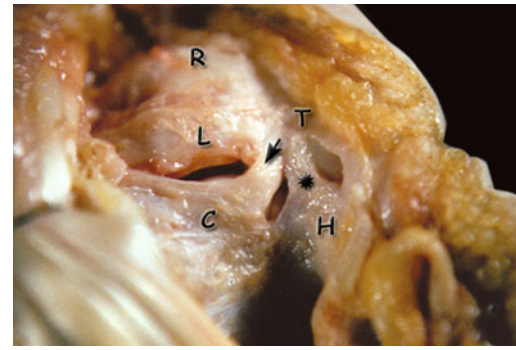

Fig. 2.12 Anatomical specimen indicating: triquetrocapitate ligament (*arrow*); triquetrohamate ligament (*asterisk*); (*C* capitate, *L* lunate, *T* triquetrum, *H* hamate, and *R* radius). With permission from [157]

onto the volar waist of the capitate without any attachment to the trapezoid (Fig. 2.10). The anatomical description and its functional significance were made by Moritomo et al. [37]. This ligament appears to deepen the socket of the STT joint and serves as a labrum for the distal pole of the scaphoid, reinforcing the palmar aspect of the STT joint capsule. It was found to be highly variable in its development. The width of the C–Tm ligament ranges from 0 to 7.7 mm (average length, 3.3 mm). The development of C–Tm ligament was directly correlated to the range of scapholunate angle and the prevalence of degenerative changes in the STT joint [37].

Triquetrocapitate Ligament (TC ligament)

The TC ligament attaches proximally to the volar and radial edges of the triquetrum. It passes obliquely distally and radially to contribute to the ulnar half of the midcarpal joint capsule before attaching to the proximal and ulnar half of the capitate body (Figs. 2.11 and 2.12). Insufficiency of the TC ligament contributes to the development of ulnar or anteromedial midcarpal instability (CIND type) [47]. It may also contribute to the constraint of midcarpal supination [4], while it is involved in the formation of the antisupination sling [43]. The yield strength has been estimated at approximately 110 N, with a yield strain at approximately 60 %.

Triquetrohamate Ligament (TH ligament)

The TH ligament is the ulnar-most ligament of the palmar midcarpal joint, originating proximally from the distal margin of the palmar cortex of the triquetrum, just ulnar to the TC ligament. It courses distally to attach to the palmar cortex of the body of the hamate, just radial to the base of the hamulus [48], with no substantial insertion onto the proximal pole of the hamate [3] (Figs. 2.11 and 2.12). The fibers of the TC and TH ligaments are interdigitated with the fibers of the UC ligament and together form the ulnar limb of the arcuate ligament. Nakamura et al. [49] described the anatomic relation of the TC and the TH ligaments as dependent on the type of lunate, whereby in type I there is no medial hamate facet and in type II there is a medial hamate facet. The relation between the TC and the TH ligaments was classified into three types. In type A, the TC ligament is completely separate from the TH ligament; in type B, the TC ligament overlaps the TH ligament; and in type C, the TC ligament has an additional ligament from the triquetrum to the proximal pole of the hamate. Eighty-two

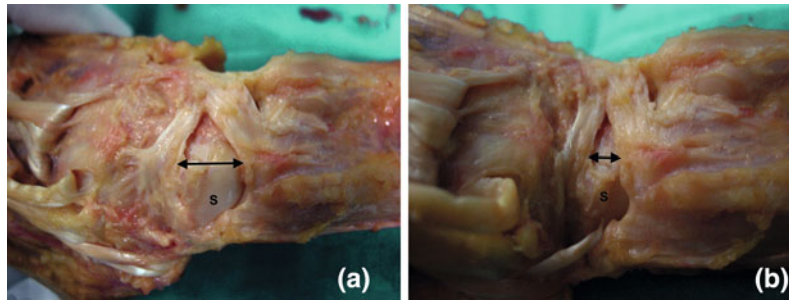

Fig. 2.13 Change in the configuration of the dorsal V ligament (dorsal radiocarpal and midcarpal ligaments) during wrist palmarflexion (**a**) and dorsiflexion (**b**), provides indirect stability to the scaphoid [52] (*S* scaphoid)

percent of type I lunates are associated with a type A relation between the TC and the TH ligaments, and 96 % of type II lunates are associated with a type C relation between the TC and the TH ligaments.

Palmar scaphotriquetral ligament (Palmar ST ligament)

There were reports of the existence of this ligamentous structure by Gunther in 1841 and Poirier et.al in 1908, (quoted by Sennwald [8]), while a more accurate description was made by Sennwald et al. [50].

Its attachment to the triquetrum is substantial and more distinct and lies between the attachments of the TC and LT interosseous ligaments. It courses horizontally spanning the midcarpal joint and inserts to the scaphoid with a thin and fan-shaped attachment, with its fibers interdigitating with those of the RSC ligament (Fig. 2.11). The palmar ST ligament may be considered an integral part of the midcarpal arcuate ligament formed by the RSC and UC ligaments [4]. With the wrist in dorsiflexion the palmar ST ligament tightens, while in palmarflexion it slackens. Radioulnar deviation does not alter the tension of the ligament. Although its function needs further investigation, it is postulated that it supports the head of the capitate during dorsiflexion of the wrist, acting as volar labrum for the lunocapitate joint [51]. It is also speculated that widening of the SL joint during dorsiflexion of the wrist, may only be possible when the palmar ST ligament is torn [50].

2.1.3 Extrinsic or Capsular Ligaments: Dorsal Surface

Until recently, emphasis was given to the description and functional significance of the palmar ligaments of the wrist. In addition, the dorsal ligaments of the wrist were generally neither preserved nor repaired during or after a dorsal approach to the wrist joint [21]. In recent years, much interest has been focused on anatomic varieties and functional significance of dorsal carpal ligaments. The dorsal radiocarpal joint is reinforced by a single ligament which bridges the ulnar half of the dorsal capsule, while the radial half of the radiocarpal joint capsule lacks any ligament reinforcement, thus leaving the proximal pole of the scaphoid and scapholunate joint uncovered. Viegas et al. [52, 53] described the "lateral V configuration" of the dorsal intercarpal and dorsal radiocarpal (DRC) ligaments. They stated that these two ligaments together act effectively as a dorsal radioscaphoid ligament that has the ability to vary its effective length threefold by changing the angle between the two arms of the V, such that the intersection angle between them at the triquetrum is acute in extension and becomes almost orthogonal in wrist palmarflexion. This ligamentous arrangement allows normal carpal kinematics while maintaining its indirect dorsal stabilizing effect on the scaphoid throughout the range of motion of the wrist. (Fig. 2.13a, b). Both dorsal ligaments, (DRC and DIC), have also been described as the dorsal V ligament [8].

2.1.3.1 Radiocarpal Joint

Dorsal Radiocarpal Ligament (DRC ligament) (Dorsal Radiotriquetral Lig., Dorsal Radiolunotriquetral Lig.)

The DRC ligament originates from the ulnar and dorsal portions of the distal end of the radius just distal and ulnar to the Lister's tubercle. It courses obliquely distally and ulnarly and inserts on the dorsal tubercle of the triquetrum. During its course it was found to have an osseous attachment onto the distal ulnar aspect of the dorsal lunate and dorsal portion of the lunotriquetral interosseous ligament (LTI ligament) [4, 20, 21]. The DRC ligament forms the floor of the fourth, fifth, and sixth extensor tendon compartments [3].

The DRC ligament morphology presents itself with many anatomical varieties [5]. It has been described as being formed by two components: a superficial radiotriquetral band and a deep radiolunotriquetral ligament, which intermingles with fibers of the lunotriquetral ligament [54]. Shaaban and Lees [55] showed that the DRC ligament consisted of two distinct parts. The ulnar part is more superficial and arises from the distal part of the interosseous border of the radius. It runs obliquely distally and ulnarward, over the distal ulna to attach to the lunate and triquetrum. On its course, the DRC ligament blends with the underlying dorsal radioulnar ligament. The radial part of the DRC ligament is deeper and arises from the posterior edge of the distal border of the radius and runs nearly horizontally and ulnarwards to attach to the lunate and triquetrum.

Mizuseki and Ikuta [56] and subsequently Viegas et al. [52, 53] classified the DRC ligament into four subtypes according to its morphology, while Smith [57] using three-dimensional Fourier transform MR imaging techniques, differentiated the DRC ligament into two subtypes. A common feature of all these subtypes is that there are forms of DRC ligament with deltoid fibers covering the dorsal aspect of the proximal scaphoid, which may offer some dorsal support to the scaphoid (Fig. 2.14).

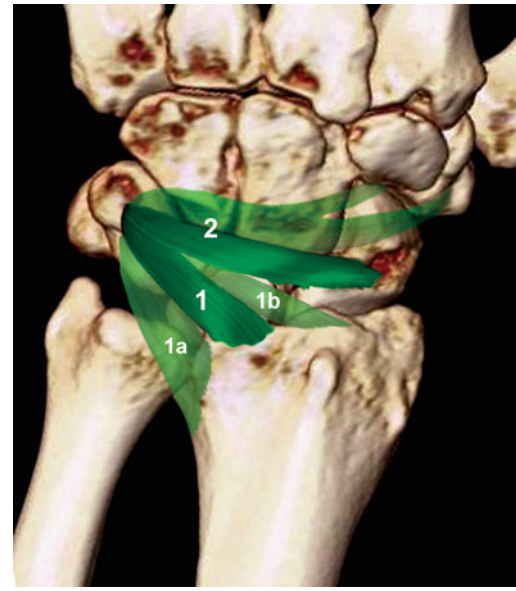

Fig. 2.14 The dorsal carpal ligaments: Dorsal radiocarpal ligament (*1*). The faint ligamentous drawings on either side of the main ligament have been described as variations: (*1a*) [55] and (*1b*) [53, 56]. Dorsal intercarpal ligament (*2*): It is consisted of a proximal thicker part (dorsal scaphotriquetral ligament) which is attached consistently to the dorsal lunate and scaphoid and a thinner distal part with inconsistent osseous attachments to the capitate, trapezoid, and trapezium [52, 57]

The reported functions of the DRC are:

(a) The DRC ligament having an oblique direction (like the palmar RC ligaments) serves to constrain ulnar translocation of the carpus [4, 13].
(b) It functions as a stabilizer and pronator of the wrist. When the forearm pronates, the DRC ligament draws the attached carpus and hand passively into pronation [22].
(c) It has been stated that the DRC ligament provides resistance to passive supination of the radiocarpal joint [10], thus participating in the formation of the antisupination sling.
(d) Sectioning the DRC ligament alters scaphoid and lunate kinematics during dynamic wrist motion and this angular change in carpal kinematics can vary up to 8° [58].
(e) The attenuation or disruption of the DRC ligament have been implicated in the

development of a static VISI deformity, either as a CIND instability [59] or as a complex instability (combination of CID and CIND instabilities), when associated with rupture of the LTI ligament [59, 60].

(f) The superficial ulnar part of the dorsal radiocarpal ligament may play a role in the stabilization of DRUJ and supporting its capsule, especially in extreme pronation [55].

2.1.3.2 Midcarpal Joint

Dorsal Intercarpal Ligament (DIC ligament)

The osseous attachments of the DIC ligament have been described by a number of authors using anatomical dissections [3, 4, 52, 54], 3-D Fourier transform MRI techniques [57] or a combination of dissection, CT imaging, and a 3-D digitization technique [20, 61]. Depending on the size of development, osseous attachments, and morphology, Viegas et al. [52] identified three types of DIC, while Smith [57] recognized four types which are comparable. The fact is that the DIC ligament originates from the dorsal surface of the triquetrum interdigitating with the fibers of DRC ligament. Coursing radially, it is constituted of a thicker portion, which inserts on the dorsal groove of the scaphoid and a thinner arm, which inserts onto the dorsal trapezium and trapezoid. The proximal thicker branch augments the dorsal regions of the LT and SL interosseous ligaments, also having osseous attachments to the dorsal lunate and scaphoid. This proximal thicker band is called *dorsal scaphotriquetral ligament* [4] and probably has an important role in the transverse stabilization of the proximal carpal row [3, 54]. It may also function as a labrum for the head of the capitate and the proximal pole of the hamate dorsally, deepening the midcarpal joint, just as the Palmar ST ligament does volarly [3, 4] (Fig. 2.14). The width of this ligament is inconstant, causing it to be frequently confused with the DIC ligament [62]. Recently, the osseous attachment of the DIC ligament on the scaphoid gained particular functional significance [63]. The most dorsal and ulnar nonarticulating part of the scaphoid, where the dorsal SL interosseous ligament and the proximal fibers of the DIC ligament attach, is called *scaphoid apex*. It is argued that carpal instability following scaphoid nonunion is closely related to whether the fracture line passes distal or proximal to the scaphoid apex [64]. Moritomo et al. [19] stated that there are two clear patterns of the interfragmentary motions of the scaphoid, based on the fracture location: the unstable (mobile) type scaphoid nonunion, where the fracture is located distal to the scaphoid apex and the stable type, where the fracture is located proximal to the scaphoid apex [19].

Its dimensions were calculated, using CT and an imaging cryomicrotome, and it was found to be approximately 1.2 mm thick, 32.6 mm long, and 6.3 mm wide [6].

Viegas et al. [52] suggested that the mechanical strength of the DIC ligament is 115.0 $\pm$ 57.2 N and that the combined mechanical properties of the DIC and the dorsal SLI Ligament have mechanical strength (162.4 $\pm$ 64.7 N) comparable with the DRC (143.3 $\pm$ 41.5 N).

Significant observations related to the DIC ligament are the following:

(a) The utilization of the DIC ligament for dorsal capsulodesis of the scaphoid in cases of scapholunate dissociation, as opposed to the traditional Blatt's capsulodesis which tethers the scaphoid to the distal radius and predictably leads to limitations in wrist flexion. The DIC ligament capsulodesis has been used by detaching the ligament off its insertion on the trapezoid and trapezium and tied to a bony trough on the dorsal surface of the distal pole of the scaphoid [65, 66]. The technique assumes that a substantial part of the DIC ligament is attached to the trapezio-trapezoid bones. Alternatively, the proximal part of the DIC ligament could be detached from the triquetrum and transferred to the distal radius after the reduction of the scaphoid malalignment [67]; (b) the need to reattach the DIC ligament to the dorsal pole of the scaphoid and lunate as well as the dorsal portion of the SL ligament in cases of static DISI [52, 68, 69]; (c) the surgical approach to the dorsum of the wrist that spares both the dorsal

radiocarpal and intercarpal ligaments [4, 70] or the concomitant ligament and nerve sparing approach [71]; and (d) having an important role in the transverse stabilization of the proximal carpal row and being part of the ligamentous arrangement which constitutes the antipronation sling, there is often a need for substitution of the DIC ligament, using tendon grafts [24].

2.1.4 Intrinsic Ligaments

2.1.4.1 Interosseous Ligaments of the Proximal Carpal Row

The scapholunate and lunotriquetral interosseous ligaments of the proximal carpal row are both C-shaped spanning the dorsal, proximal, and palmar margins of their respective joint spaces [48]. Their integrity is essential for maintenance of normal carpal kinematics. The thickest and strongest region of the scapholunate ligament is located dorsally, while that of the lunotriquetral ligament is located palmarly [72, 73]. This construction seems to support the "balanced lunate" concept [73], meaning that the lunate is under the influence of two opposite moments (scaphoid flexion and triquetral extension) which counteract each other (Fig. 2.15).

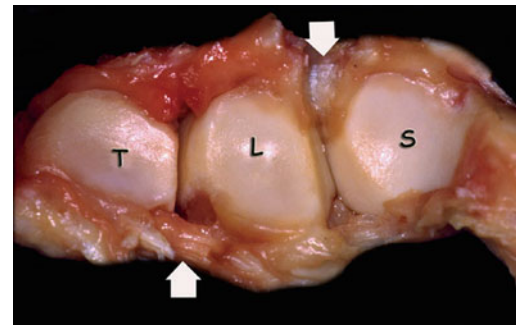

Fig. 2.15 The distal articular surfaces of the proximal carpal row bones as seen from the midcarpal joint. The distal parts of the scapholunate and lunotriquetral joint spaces remain free from ligamentous attachments. *White arrows* indicate the strongest regions of the scapholunate (dorsal) and the lunotriquetral (volar) ligaments. (*S* scaphoid, *L* lunate, *T* triquetrum). With permission from [157]

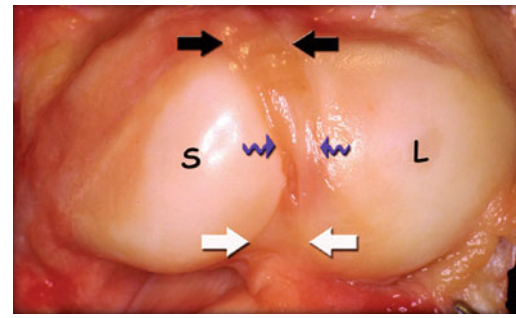

Fig. 2.16 The scapholunate interosseous ligament as seen from the radiocarpal joint. Dorsal region (*black arrows*); Volar region (*white arrows*); proximal fibrocartilaginous region (*wavy blue arrows*) (*S* scaphoid, *L* lunate). With permission from [157]

Scapholunate interosseous ligament (SLI ligament)

The SLIL has been described as consisting of three regions on the basis of macroscopic and histological criteria: dorsal, proximal, and palmar regions (Fig. 2.16). Bone insertions on both the scaphoid and the lunate are limited to the most proximal and superior parts of the articular surface between the two bones [62]. The dorsal and palmar regions have histologic organizations consistent with true capsular ligaments, while the proximal region is composed of fibrocartilage, with few collagen fascicles [4]. The dorsal region is the thickest of the three regions, it has a trapezoidal shape and is composed of transversely oriented collagen fascicles surrounded by connective tissue, through which course vascular and nervous bundles. It measures approximately 5–6 mm in proximal—distal length, 3–5 mm long, and 2–4 mm thick. It is contiguous distally to the dorsal scaphotriquetral ligament and merges proximally and indiscernibly with the proximal region of the SL ligament. The proximal region of the SL ligament can extend into the scapholunate joint space with a triangular cross-section, much like a knee meniscus. The proximal region is composed almost entirely of fibrocartilage. It is approximately 1 mm thick, 4 mm long, and 11 mm wide [20]. The continuity of the proximal and palmar regions of the SL ligament is interrupted by the RSL ligament [3]. The dimensions of the palmar region vary

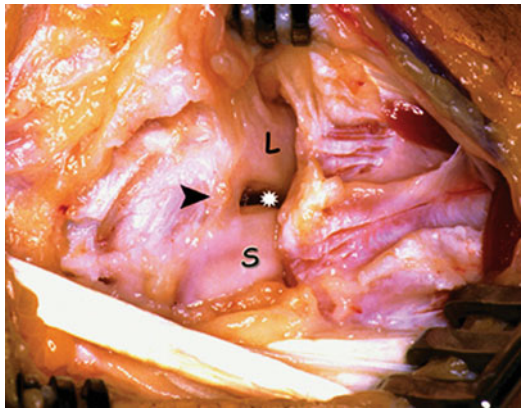

Fig. 2.17 Surgical finding of a patient, who reported pain during loading of the wrist in dorsiflexion. Watson test was negative. The dorsal SL ligament was intact (*arrow*), while the proximal region was absent due to chronic rupture (*asterisk*). (*S* scaphoid, *L* lunate). With permission from [157]

between 1 and 2 mm in thickness, 3–5 mm in length, and 4–7 mm in width [20, 25, 62]. Its fibers are obliquely oriented from the palmar rim of the proximal scaphoid to the palmar rim of the palmar horn of the lunate. This region of the ligament is not visible because the LRL ligament covers its palmar surface, while proximally and dorsally it is covered by the RSL ligament.

The SLIL is a strong ligament often requiring up to 300 N of distraction force to rupture. The majority of distraction strength is found in the dorsal region, the palmar region fails with 150 N stress, and the proximal region can withstand only a 25–50 N stress [4, 74]. Biomechanical studies showed that the dorsal region is the most critical for resistance to palmar–dorsal translation and distraction, but the palmar region is the most important rotational constraint [62, 74]. The proximal fibrocartilage region appears appropriate to accept compression and shear loads (Fig. 2.17). Less than 20° of motion is possible at the SL joint [29]. A number of biomechanical studies have emphasized the importance of the SLIL as the primary stabilizer of the SL articulation and that its disruption alters scaphoid and lunate kinematics, i.e., scaphoid flexion, scaphoid pronation, and lunate extension [75, 76].

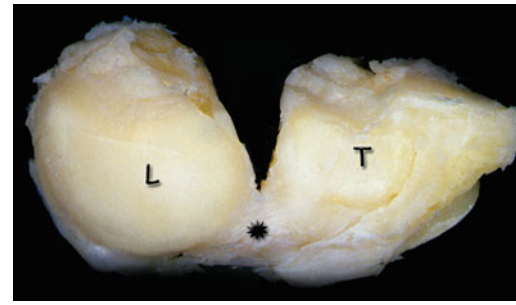

Fig. 2.18 The lunate and triquetral bones from the dorsal side. Lunotriquetral ligament (*asterisk*). With permission from [157]

It is known that the dorsal and proximal regions of the SLI ligament are the most accessible regions through a dorsal wrist arthrotomy, while it is impossible to approach the palmar region of the scapholunate ligament without compromising the palmar radiocarpal ligaments through a palmar wrist arthrotomy [74]. Regardless of the above, some authors, believing that the palmar region of the SLI ligament plays an important role in the stability of the SL complex, suggested the reconstruction of the palmar part of the ligament alone [77] or in combination with the dorsal part of the SLI ligament [78] or substituted the palmar part with tendon graft in cadavers [79]. Berger [74, 80] suggested that for scapholunate dissociation, the operation is unlikely to be successful with reconstruction of the dorsal SLIL alone. In addition, there are reports upgrading the mechanical [81] and sensory [82] importance of the palmar SLI ligament.

Lunotriquetral interosseous ligament (LTI ligament)

The LT ligament is divided histologically into three regions, in a manner similar to the SL ligament (Figs. 2.15 and 2.18). The dorsal and palmar regions are composed of true ligaments, with collagen fascicles, perifascicular spaces, small blood vessels, and nerves. The proximal region is composed of avascular fibrocartilage [4]. The palmar subregion of the LT ligament is the thickest subregion (2.3 ± 0.3 mm) and the proximal region is the thinnest (1.0 ± 0.2 mm); the

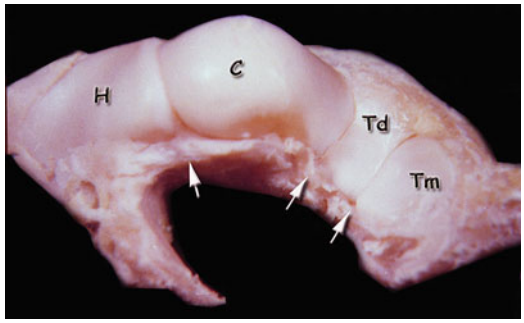

Fig. 2.19 The proximal articular surfaces of the distal carpal row. *Arrows* indicates the volar interosseous ligaments of the distal carpal row. (*H* hamate, *C* capitate, *Td* trapezoid, *Tm* trapezium). With permission from [157]

dorsal subregion is intermediate (1.4 ± 0.2 mm) [73]. The dorsal region is often reinforced with fibers of the DRC and dorsal scaphotriquetral ligaments.

The palmar region is strongly reinforced and interdigitating with fibers from the UC ligament. The proximal region, like the SLIL, resembles a knee meniscus, often with a distally directed apex extending into the LT joint space.

The material and constraint properties have shown that the palmar component failure force was 301 ± 36 N; the dorsal, 121 ± 4 2 N; and the proximal, 64 ± 14 N [73].

Contrary to the SLIL, the palmar region of the LTI is the most critical in constraining mutual translation of the lunate and triquetrum, whereas the dorsal region is the most important rotational constraint.

Published reports have shown that isolated complete sectioning of the LT ligament alters the kinematics of the LT complex, but the classic VISI deformity does not occur until both the dorsal radiotriquetral (RT) and scaphotriquetral (ST) ligaments are compromised [4, 83].

2.1.4.2 Interosseous Ligaments of the Distal Carpal Row

The four bones of the distal carpal row form three interposed joints: trapezium-trapezoid, trapezocapitate, and capito-hamate joints. These joints are principally constrained by ligaments that simply span the joint space of two adjacent bones. These joints are bridged by interosseous ligaments and adjoin each other especially on the palmar side (Fig. 2.19). These ligaments do not span the entire proximal–distal dimension of the joint, having only dorsal and palmar portions, which tend to interdigitate with fibers from the adjacent carpometacarpal joints [4].

It has been stated that the interosseous ligaments (especially their palmar regions) connecting the bones of the distal carpal row, are crucial in providing transverse carpal stability and that the flexor retinaculum has small contribution to the transverse carpal stability [84].

Trapeziotrapezoid ligament (TT ligament)

The TT ligament is composed of dorsal and palmar regions transversely spanning the dorsal and palmar edges of the trapezium-trapezoid joint space. Both regions are 1–2 mm thick and up to 5 mm wide in the proximal–distal direction. The dorsal region forms the floor for the ECRL tendon. The material properties of the dorsal and palmar regions have been studied, revealing yield strengths of 150 and 125 N, respectively [15].

Trapeziocapitate Ligament (TC ligament)

The TC ligament is composed of dorsal, palmar, and deep regions. The dorsal and palmar regions are composed of flat sheets of true capsular ligament (1–2 mm thick, 3–5 mm wide), spanning the space between the two bones.

The deep region is situated entirely within the joint space; it is cylindrical in shape and covers the "notch" created in the articular surface of the trapezoid and capitate. The deep component substantially enhances the structural integrity of the joint. Material property testing of the dorsal and palmar regions of the TC ligament reveal failure occurring at approximately 125 N individually [15, 84].

Capitohamate Ligament (CH ligament)

The CH ligament, like the TC ligament, can be divided into three regions—dorsal, palmar, and deep. The dorsal region is thick (1–2 mm) and broad and is transversely oriented, spanning the

distal part of the capitohamate joint. The proximal part of the joint is devoid of ligamentous connections. The dorsal region was found to be the principal stabilizing structure for palmar rotation and palmar translation, as well as for proximal and distal translation of the capitate relative to the hamate. The palmar region is similar to the dorsal, but is more continuous with the other palmar interosseous ligaments. The deep region was found to be short and very strong while, because of its central location to the joint, it acts as a pivot point for rotation at the CH joint. It is most important in constraining dorsal rotation and dorsal translation of the capitate relative to the hamate. The coherence between capitate and hamate was investigated by Ritt [83], who found that the dorso–palmar translational displacement averaged 0.9 and 0.5 mm, respectively, proximal–distal translational displacement averaged 0.8 and 0.4 mm, respectively, and distractional displacement averaged 0.3 mm. Material property studies reveal that the deep ligament was strongest at 289 N, followed by the palmar at 171 N and the dorsal at 133 N [83].

Therefore, the CH ligament and especially the combined palmar and deep regions exhibit the greatest strength contributing substantially to the transverse stability of the distal row.

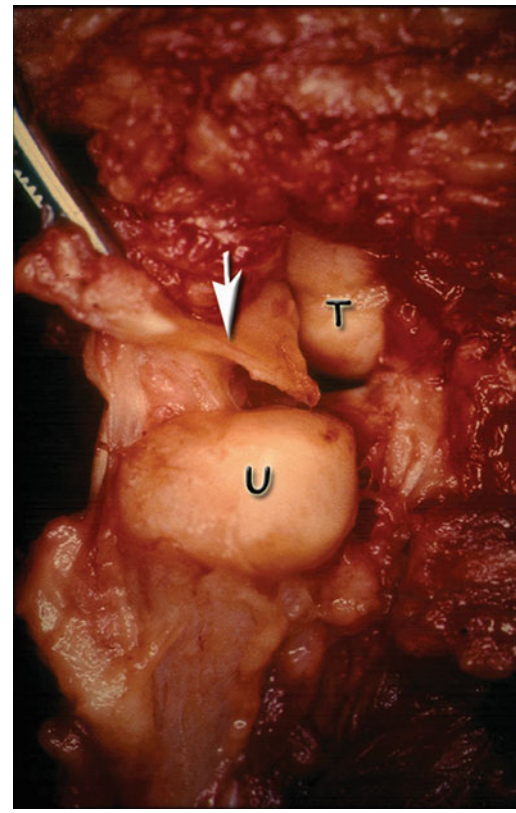

Fig. 2.20 The distal radioulnar joint. The *arrow* indicates the articular disk, which has been cut from the sigmoid notch and lifted up. *U* ulnar head, *T* triquetrum. With permission from [157]

2.1.5 Ligaments of the Distal Radioulnar Joint

2.1.5.1 Triangular Fibrocartilage Complex

The triangular fibrocartilage complex (TFCC) separates DRUJ from the radiocarpal joint. The term "TFCC" was invented by Palmer and Werner [85]. The complex includes: the articular disk (discus articularis) (Fig. 2.20), the dorsal and palmar radioulnar ligaments, the meniscus homologue (MH), and the extensor carpi ulnaris sheath (the floor of which is often called the ulnar collateral ligament) (Fig. 2.21). The TFCC originates from the distal rim of the radial sigmoid notch and inserts on the fovea of the ulnar head and the base of the ulnar styloid. The articular

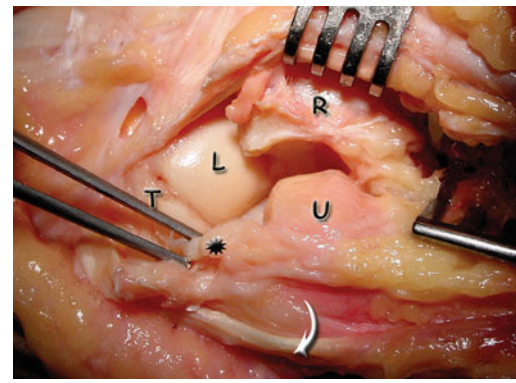

Fig. 2.21 DRUJ from the dorsal side. The picture indicates the close relationship of the ECU sheath with the TFCC. The ECU tendon has been dislocated from its sheath (*curved arrow*). The *asterisk* indicates the TFC that has been lifted off its radius attachment. *T* triquetrum, *L* lunate, *U* ulnar head, *R* radius. With permission from [157]

disk is a fibrocartilaginous biconcave structure, interposed between the ulnar dome and the ulnar aspect of the carpus. Although it has been determined that the thickness of the articular disk proper is generally 1–2 mm, the thickness varies inversely with positive ulnar variance [86].

The dorsal (DRU) and palmar (PRU) radioulnar ligaments are composed of longitudinally oriented bundles of collagen fibers that originate and insert directly into the bone, while the central articular disk is composed of fibrocartilage that originates from the hyaline cartilage of the distal radiolunate fossa [87, 88].

The DRU and PRU ligaments, contribute to the formation of the extensor carpi ulnaris subsheath and the ulnocarpal ligament complex, respectively [3]. The DRU ligament is also reinforced with ligamentous fibers originating from the ulnar aspect of the distal radius. These ligamentous fibers have been described as a separate ligament (dorsal radial metaphyseal arcuate ligament [48]), a component of the dorsal radiocarpal ligament [55], or part of the interosseous ligament of the forearm [89].

The DRU and PRU ligaments consist of *superficial* components inserting directly onto the ulna styloid and *deep* components inserting more lateral, into the fovea adjacent to the articular surface of the pole of the distal ulna [90] (Fig. 2.22). The fibers of the superficial component form an acute angle as they converge on the ulna styloid from the medial radius. This acute angle of attachment gives the superficial TFC a poor mechanical advantage for guiding the radio-carpal unit through an arc of pronosupination. The deep components of the TFC form an obtuse angle of attachment, much more mechanically advantageous in stabilizing rotation of the radius around the fixed ulna. The deep components of the TFC have been referred to by wrist investigators as the *Ligamentum subcruentum* [30, 90, 91].

Two independent studies, that of Af Ekenstam and Hagert [92], Schuind et al. [93], have created confusion in the scientific community as to which fibers (those of DRU or PRU ligament) tighten in pronation and which tighten in supination, because the results of their study were exactly the opposite. The conflict ended in 1994 when Hagert [94] recognized that both research groups were correct but that each was examining a different piece of the puzzle. Af Ekenstam and Hagert [92] examined the deep fibers, while Schuind [93] examined the superficial fibers of the ligaments. Hagert [94] clearly stated that in forearm pronation, the dorsal superficial fibers of the TFC must tighten for stability, as do the deep palmar fibers of the Ligamentum subcruentum. Conversely, in supination, the palmar superficial TFC radioulnar fibers (to the ulna styloid) tighten, as do the deep dorsal fibers of the Ligamentum subcruentum, making both theories correct.

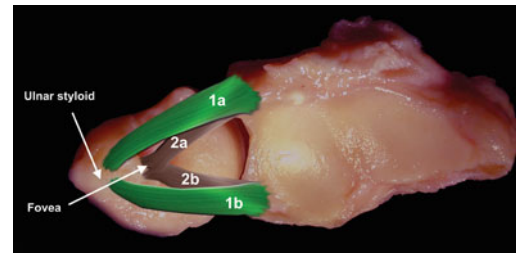

Fig. 2.22 The superficial components of the dorsal (*1a*) and volar (*1b*) radioulnar ligaments that are inserted to the ulnar styloid; the deep components of the dorsal (*2a*) and volar (*2b*) radioulnar ligaments, which are inserted to the fovea of the ulnar head. Both components (*1a* and *2a*) constitute the dorsal radioulnar ligament, while both (*2a* and *2b*) components constitute the volar radioulnar ligament

The radius of curvature of the sigmoid notch is 15 mm and its center correlates to the ulnar styloid, while the radius of curvature of the ulnar head is 10 mm and its center correlates to the region of the fovea. This difference in the radius of curvatures leads to both rotational and sliding motions in the normal joint.

Hagert and Hagert [95] recently presented a new perspective on the stability of the joint which is correlated to the structural principle named *Tensegrity (A term derived from combining the words tension and integrity; means that the integrity of a structure depends on the balance of tension and compression within it)*. The analogue of this principle to the stability of DRUJ is that "the radioulnar ligaments have a spiral configuration as they insert into a surface area, not one single point, on the ulnar head. The helicoidal

bundles, in conjunction with the combined centric and epicentric insertions of the deep and superficial radioulnar portions respectively, lead to a continuous shift in the tension of various portions of the ligaments. This continuous shift in tension and compression constitutes the core of DRUJ stability and is the essence of tensegrity".

The Meniscus Homologue (MH) is the soft-tissue structure that emerged after the recession of the ulnar styloid in hominoids [30]. The MH has been described as a triangular soft tissue structure located in the space between the medioproximal aspect of the triquetrum and the ulnar styloid process and the articular disk. It is formed by well vascularized, loose connective tissue, the inner surface of which is lined by synovial cells. Although it has been considered as an extension of the TFC [96] or as a true collateral ligament [97], Berger [3] stated that the impression of a "meniscus" is derived from paracoronal sections of cadaver wrists, where the section cuts were through the prestyloid recess, where the UT ligament appears to form a distal "lip" covering the recess and that in any case it does not denote any functional significance or anatomic difference from surrounding tissue.

According to Ishii et al. [91]. the MH and the prestyloid recess (the cavity adjacent to the ulnar styloid) can be seen in three anatomic variations: the narrow opening type in 74 % of specimens, the wide opening type in 11 %, and the no opening type in 15 %.

The TFC receives its blood supply from: (1) the ulnar artery through its palmar and dorsal radiocarpal branches and (2) the dorsal and palmar branch of the anterior interosseous artery [87, 98]. Interosseous vessels from the ulnar head also enter the TFCC through the foveal area. Small vessels penetrate the TFCC in a radial fashion from the palmar, ulnar, and dorsal attachments of the joint capsule and supply the peripheral 10–20 % of the TFC. The central 80–85 % is avascular, with no vessels entering the articular disk from the radius [87, 99]. Therefore, tears that occur in the center and along the radial attachment of the disk, are not likely to heal [98, 99].

The TFCC has been shown to have three major functions:

1. The central part (articular disk) functions as a cushion for the ulnar carpus carrying approximately 20 % of the axial load of the forearm.
2. The peripheral part (ligamentous) is the major stabilizer of the DRUJ.
3. The ulnocarpal ligaments and the sheath of the ECU contribute to the stability between the ulnar head and the ulnar carpus.

2.1.6 Morphology and Ligamentous Restraints of the Scaphoid

Many authors clearly demonstrated the variations in morphology of the carpal bones and their articulations [100–102]. Normal carpal kinematics relies on the complex interplay between the arrangement of carpal ligaments and carpal bone morphology [103], while the ligamentous attachments of the scaphoid and the shape of the bones with which it articulates, play an important role [104, 105].

The morphological and morphometric features of the scaphoid have been described in radiographs [106], and in cadavers [107, 108]. Although the ligament attachments cover 9 ± 0.9 % of the total scaphoid surface area, there is a lack of consensus on the anatomy of the ligaments attaching to the scaphoid, while interindividual variability of ligament insertions and morphology, exists [5].

In vivo kinematic studies had previously identified two distinct types of scaphoid motion [109–111], which constitute two major theories of carpal mechanics (row and column). In both theories, the scaphoid is considered an essential structure [104, 112], but the patterns observed have not been related to anatomical variations in the reviewed literature [113]. Fogg [113] in his thesis correlated the anatomic variation in morphology of the scaphoid and of the ligaments attached to it, with the kinematic behavior of the scaphoid. The two types of scaphoid are summarized in Table 2.2.

Table 2.2 Osseous and ligamentous characteristics of the two types of scaphoid

	Type 1 scaphoid rotating/translating. Row theory	Type 2 scaphoid flexing/extending. Column theory
Osseous morphology		
Dorsal crest	Single dorsal high crest	Three dorsal low crests
Distal articular surface	Large and elongated	Small
Ulnar surface to capitate	Large, elongated, and shallow	Short and deep; Acts as fulcrum about which the scaphoid is moved
Ulnar surface to lunate	Smaller	Larger
Length of scaphoid	Longer	Shorter
Tuberosity	Prominent tuberosity	Less distinct tuberosity
Ligamentous patterns		
STT ligament	V-shape with proximal apex	V-shape with distal apex
Scaphocapitate lig	Long and thin; radial scaphoid attachment	Short and wide; ulnar scaphoid attachment
Dorsal intercarpal lig	Trapeziotrapezoid radial attachment	Scaphoid radial attachment
Radiocapitate lig.	No scaphoid attachment (Radiocapitate lig.)	Scaphoid attachment (Radioscaphocapitate lig.)

It is widely accepted that the ligamentous restraints stabilizing the scaphoid are classified into primary and secondary [41, 42, 58, 114–116]. There is no consensus as to which ligaments are the primary and which are the secondary stabilizers. SLIL is considered as *the primary stabilizer* of the SL joint and is surrounded by several secondary stabilizers, each insufficient to cause instability after isolated disruption, but each is important in the maintenance of normal SL kinematics and vulnerable to attritional wear after complete disruption of the SLIL [116]; this is thought to be the etiology for delayed development of dorsal intercalated segment instability (DISI) after isolated disruption of the SLIL. The relative importance of each of these ligaments to SL stability has not conclusively been established; however, the status of the secondary stabilizers is particularly important in choosing the method to treat the SL instability.

As *Scaphoid secondary stabilizers* or the second line of defense, the following have been reported: the STT, RSC, SC, and the unique V-arrangement of the DIC and DRC ligaments. Probably the insertions of the DIC (dorsal scaphotriquetral ligament) to the dorsal SLIL and its osseous attachments to the dorsal lunate and scaphoid should also be considered as primary stabilizers of the scaphoid.

In clinical settings, there are cases of rupture or insufficiency of the primary ligamentous restraints, while the secondary restraints are intact. Such cases manifest with *SL dissociation without rotary subluxation of the scaphoid (RSS)* (widening of the SL space, rupture of the dorsal SL ligament, and normal SL angle) (Fig. 2.23a, b, c). At the other end of the spectrum, there are cases with insufficiency mainly of the secondary stabilizers, while the primary stabilizers remain relatively intact. Such cases manifest with *RSS without SL dissociation* (foreshortened scaphoid on posteroanterior radiographs with a positive ring sign, increased SL angle, and the dorsal SL ligament macroscopically intact) (Fig. 2.24a, b, c). Finally, there are cases of concurrent injury of the primary and secondary stabilizers which is manifested *with SL dissociation and RSS* resulting

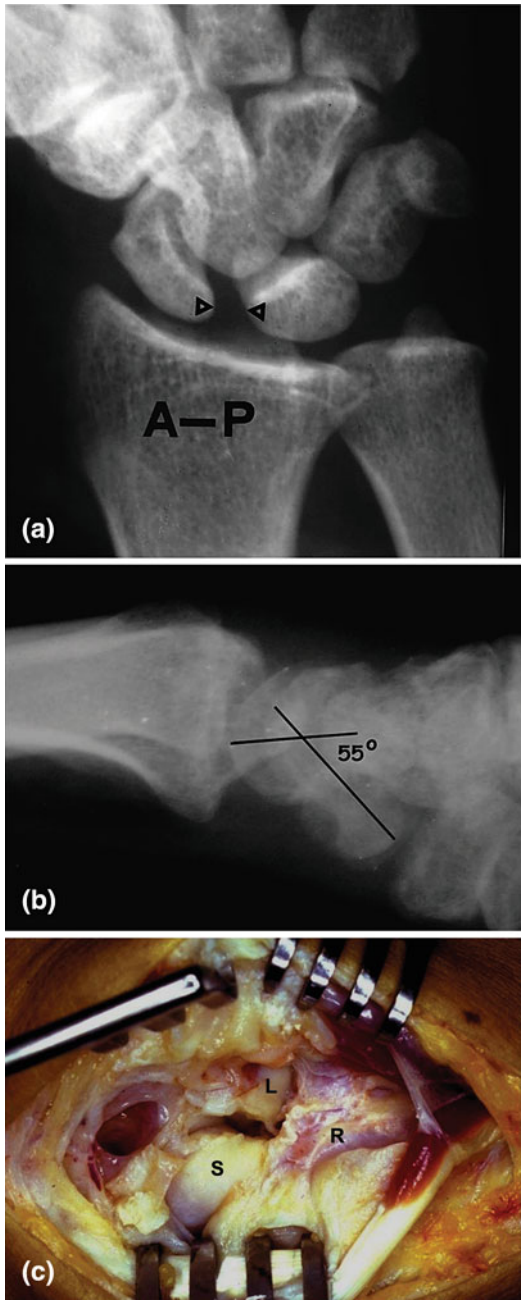

Fig. 2.23 An example of injury of the primary ligamentous restraints of the scaphoid, while secondary restraints are intact. Widening of the SL space (**a**), normal SL angle (**b**), complete rupture of the dorsal SL ligament (**c**)

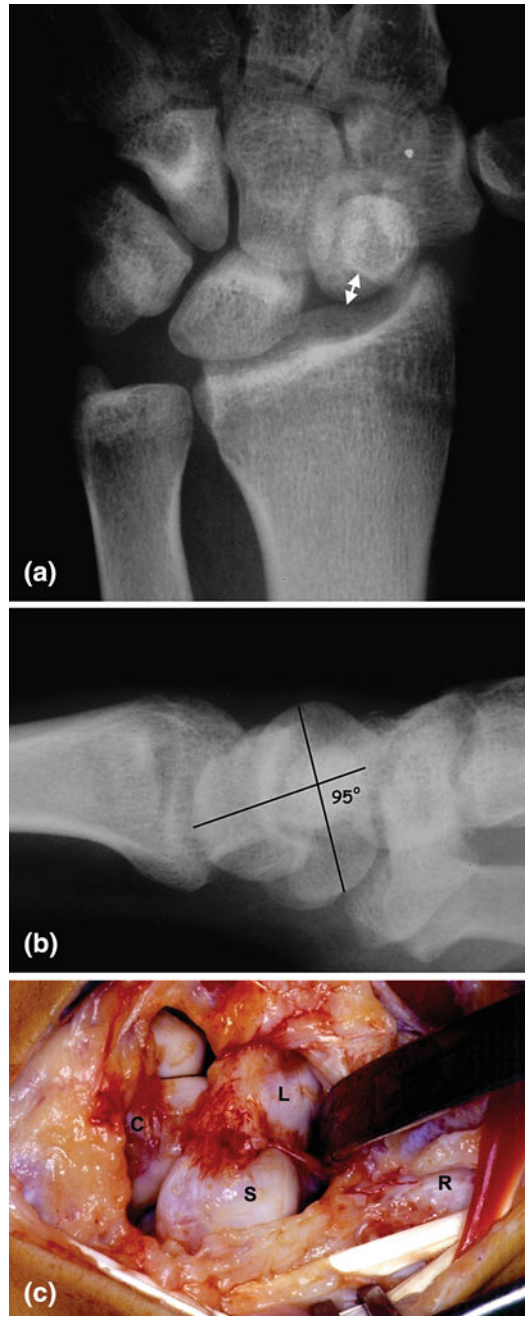

Fig. 2.24 A case with insufficiency of the secondary stabilizers while the primary stabilizers remain relatively intact. Foreshortened scaphoid on P-A radiographs with a positive ring sign (**a**), increased SL angle (**b**) and a macroscopically intact dorsal SL ligament (**c**)

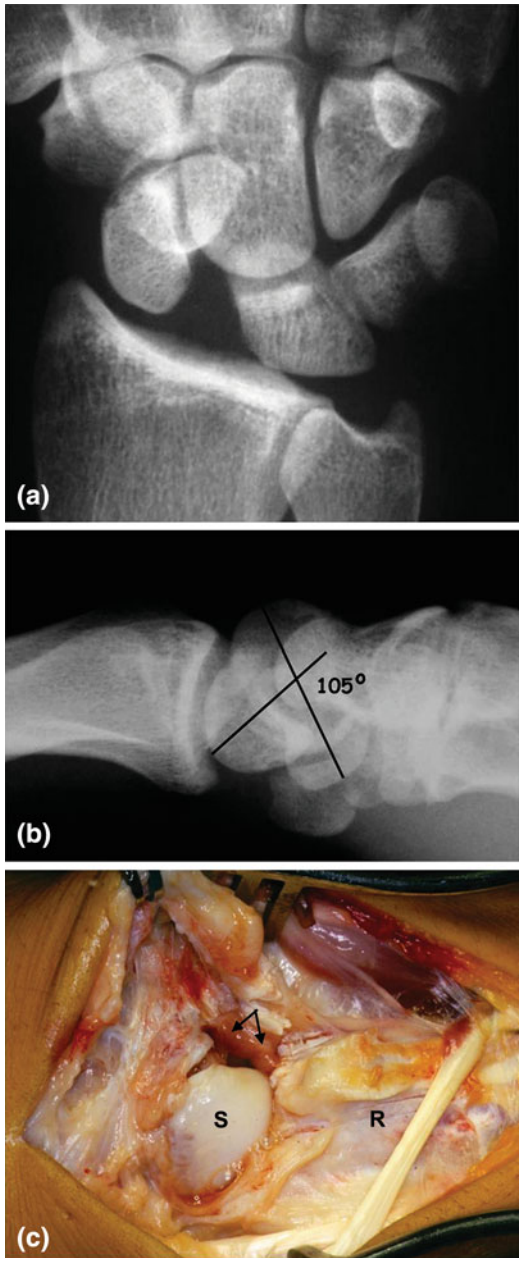

Fig. 2.25 A case of concurrent injury of the primary and secondary stabilizers of the scaphoid. SL dissociation (**a**), rotatory subluxation of the scaphoid (**b**) and complete rupture of the SL ligament (**c**)

either because the initial injury is extensive or because to the initial limited ligamentous injury, attritional wear or slackening of the remaining ligaments is added (Fig. 2.25a, b, c).

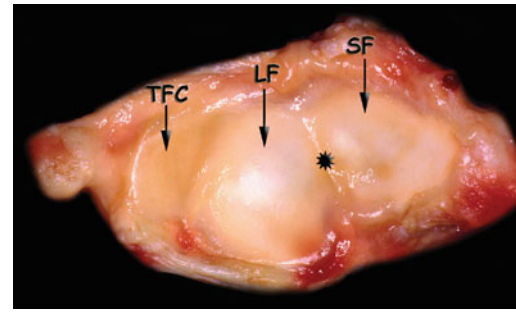

Fig. 2.26 The proximal part of the radiocarpal joint. Scaphoid fossa (*SF*), lunate fossa (*LF*), triangular fibrocartilage disk (*TFC*), interfacet prominence (*asterisk*). With permission from [157]

2.2 Anatomy of the Joints

2.2.1 Radiocarpal Joint

The radiocarpal joint is a glenoid type of articulation consisting of two elements: (a) the antebrachial glenoid, formed by the distal articular surface of the radius in conjunction with the TFC (Fig. 2.26) and (b) the carpal condyle, formed by the convex proximal articular surfaces of the proximal carpal row bones.

The articular surface of the distal radius is grossly triangular in shape with its apex toward the radial styloid and its base next to the articular cavity for the head of the ulna (sigmoid notch). The radius has two articular facets (the scaphoid and lunate fossae), separated by a cartilaginous saggital ridge (the interfacet prominence). The biconcave scaphoid fossa is triangular or oval shaped and has a smaller radius of curvature than that of the lunate fossa. The orientation of the scaphoid fossa is 11° volar and 21° ulnar relative to the long axis of the radius [14]. The lunate fossa is quadrangular in shape, biconcave although shallower, and less inclined toward the ulnar side (15° average) than the scaphoid fossa (30°). The volar lunate facet projects approximately 3 mm anterior to the flat volar surface of the distal radius with narrow width (on average <5 mm) [48]. The fracture of this bone protrusion (to which the SRL ligament attaches)

Fig. 2.27 The projection of the volar lunate facet

Fig. 2.28 The ulnovolar inclination of the distal radius. With permission from [157]

destabilizes the wrist, while its fixation is difficult with the usual volar plates (Fig. 2.27). The radioulnar and the dorso–palmar diameters of the two articular surfaces are 4–5 and 1.5–2 cm, respectively. The distal articular surface of the distal radius is tilted in two planes. In the saggital plane, there is an average 10° of tilt and in the frontal plane there is an ulnar inclination averaging 24° (19°–29°) [117] (Fig. 2.28).

The bones of the proximal row are joined at their proximal edges by the interosseous ligaments forming a smooth biconvex surface. Communication through these ligaments becomes a normal feature at advanced ages [96].

The thickness of the articular cartilage of the distal articular surface of the radius ranges between 0.7 and 1.2 mm. There is a significant difference in the size of the articular surfaces and the degree of curvature between the opposing articular surfaces of the radiocarpal joint. The proximal articular surfaces of the scaphoid and lunate are 60 % larger than the distal articular surface of the radius. The curvature of the proximal carpal row is 1.5 times greater than that of the distal articular surface of the radius.

It has been postulated that differences in bony anatomy of the radioscaphoid articulation may affect the scaphoid stability after soft-tissue injury. Larger curvatures of the scaphoid fossa and proximal scaphoid as well as a deeper scaphoid fossa and a greater volar tilt of the radius, are factors preventing instability despite any ligamentous tears [118].

The joint capsule is reinforced by palmar and dorsal capsular ligaments the inner side of which appears resurfaced by synovial tissue. A number of recesses, varying in size and shape, have been described: (a) recessus prestyloideus, located just palmar to the ulnar styloid process, (b) recessus prescaphoideus, located proximal and palmar to the scaphoid, (c) recessus preradialis, located in front of the RSL ligament, and (d) recessus pretriquetralis which acts as communication with the pisotriquetral joint.

2.2.2 Midcarpal Joint

From an anatomic point of view the midcarpal joint may have the most complicated joint shape in the human body. In a broad sense there are three articulations: (a) the STT joint, (b) the scapholuno-capitate joint, and (c) the triquetrohamate joint. The former is convex proximally whereas the latter two are concave.

2.2.2.1 Scapho-Trapezium-Trapezoid Joint

It is a glenoid type of joint that is formed from the convex articular surface of the scaphoid and the concave joints of trapezium-trapezoid. Moritomo et.al [37] depending on the shape, recognized three types of joint surfaces of the distal scaphoid and in most cases (81 %) they found an interfacet ridge on the joint surface of the distal scaphoid, which is oriented in line with the trapezio-trapezoid articulation (Fig. 2.29). This ridge was classified into three categories according to its

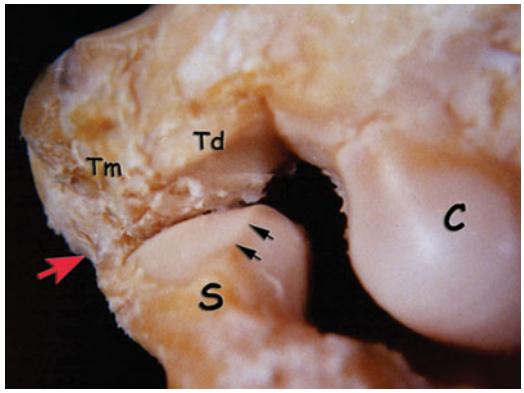

Fig. 2.29 The radial side of the midcarpal joint. The STT ligament (*red arrow*); The interfacet ridge of the distal scaphoid (*double black arrows*); (*C* capitate, *S* scaphoid, *Tm* trapezium, *Td* trapezoid). With permission from [157]

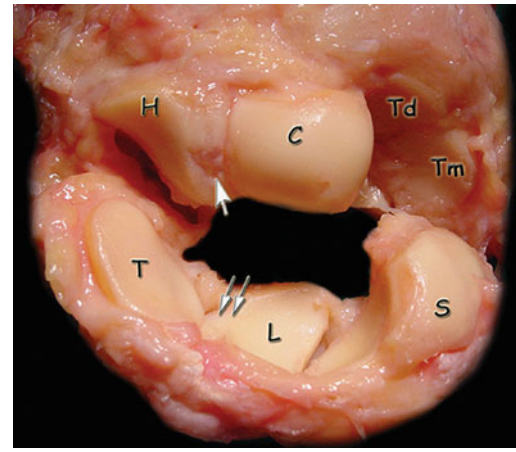

Fig. 2.30 The midcarpal joint. A lunate type II is apparent (*double arrows*) with arthritic changes of the proximal hamate (*white arrow*) (*T* triquetrum, *L* lunate, *S* scaphoid, *H* hamate, *C* capitate, *Tm* trapezium, *Td* trapezoid). With permission from [157]

development or lack of development and runs obliquely from radiodorsal to ulnopalmar dividing the distal surface of the scaphoid into two facets [37]. They suggested that the orientation of this obliquely oriented ridge guides STT joint motion and coincides with the plane of dart-throwing motion. On the contrary, it has been suggested that the ridge is merely cartilaginous, and therefore cannot resist such forces and they considered the ridge as a result of wrist motion, not a factor influencing motion [113].

2.2.2.2 Scapholunocapitate Joint

It is a ball and socket joint, formed by the concave articular surfaces of the lunate and scaphoid proximally and the convex articular surface of the capitate and sometimes the proximal pole of the hamate, distally. Two types of articular surfaces of the scaphoid that articulate with the lunate and capitate have been identified. A large lunate facet is coupled with a small, distal capitate facet, while a small lunate facet is coupled with a large, proximal capitate facet [106, 113].

In the MC joint, two types of lunates have been identified based on their distal articular surface: In type I lunates there is no medial facet, while type II lunates have a medial facet that articulates with the hamate. This is a distinctive facet with a ridge on the hamate separating it from the triquetrohamate joint and a ridge on the lunate separating it from the capitolunate joint [100]. The lunate type was determined using capitate–triquetrum (C-T) distance. A type I lunate was defined as a C-T distance $\leq$2 mm. A type II lunate was defined as a C-T distance $\geq$4 mm [119].The size of the medial facets in type II lunates ranges from 1 to 6 mm [120] and its incidence has been reported to range from 46 to 73 % [100, 102, 120].

The clinical significance of the wrists with type II lunates has been described by many authors: (a) the kinematics of a type II lunate are different from those of a type I lunate during radial-ulnar deviation of the wrist [110, 121] and the condylar double-facet midcarpal articulation permits only flexion and extension of the proximal carpal row, restricting radial translation [151]; (b) arthritic changes at the proximal pole of the hamate were more commonly associated with the type II lunates (49 %) [49], while these arthritic changes were also associated with LTI ligament tears [100] (Fig. 2.30); (c) variations in scaphoid motion of the wrists with lunate type II may contribute to the development of STT arthritis [119]; (d) type II lunates constitute an anatomical factor predisposing to Kienbock's disease, because the loads applied to the

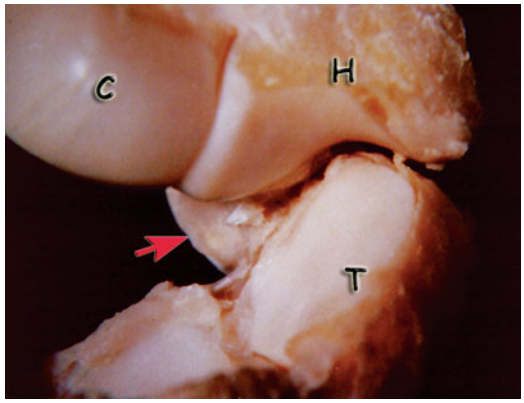

Fig. 2.31 The ulnar side of the midcarpal joint. The helicoidal shape of the articular surface of the hamate is apparent. The volar triquetrocapitate ligament (*red arrow*) (*C* capitate, *H* hamate, *T* triquetrum). With permission from [157]

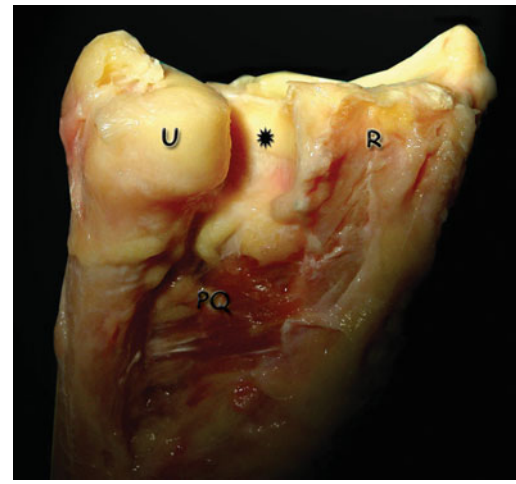

Fig. 2.32 The DRUJ from the dorsal side. (*U* ulnar head, *R* radius). Sigmoid notch (*asterisk*). With permission from [157]

radiolunate joint are supposed to be greater in type II lunates than in type I [123], and (e) type II lunate morphology is associated with significantly decreased incidence of DISI deformity in cases of established scaphoid nonunion [122].

2.2.2.3 Triquetrohamate Joint

It is a helicoid or screw shape joint, formed by the distal surface of the triquetrum and the proximal surface of the hamate (Fig. 2.31). McLean et.al [124] suggested the existence of two distinct TqH joint patterns, which have been termed TqH-1 and TqH-2. A TqH-1 joint is a helicoidal configuration. It is double faceted, with the hamate and the triquetrum articular surfaces possessing complementary concave and convex parts. A TqH-2 joint has a predominantly oval convex shape, whereas the primarily concave triquetrum is better described as a dish for the flatter hamate. It has no hamate groove or distal ridge. There appears to be a spectrum of variation between these two identifiable types.

2.2.3 Distal radioulnar joint (DRUJ)

DRUJ is a trochoid articulation, formed by the ulnar head and the sigmoid notch of the distal radius. The articular surface of the radius that articulates with the ulna is called the sigmoid notch. The sigmoid notch has a triangular shape with a distal, a dorsal, and a palmar rim. The distal rim separates the lunate fossa from the sigmoid notch and is the site of insertion of the triangular fibrocartilage disk. The portion of the ulnar head that articulates with the sigmoid notch is referred to as the "seat" and the articular surface in juxtaposition to the proximal (undersurface) of the TFCC is the "pole" (Fig. 2.32).

The arc of curvature of the sigmoid notch ranges from 47° to 80°. Articular cartilage covers a much greater arc of the ulnar head, ranging from 90° to 135°. The radius of curvature of the sigmoid notch is 15 mm, compared to 10 mm for the seat of the ulna. Thus, the ulnar head and the sigmoid notch are obviously not congruent. This incongruity between the radius of curvature of the sigmoid notch and the ulnar head results in: (a) *Reduced articular contact between the articular surfaces*. At the neutral position, approximately 60 % of the cartilage surfaces are in contact, whereas at the extremes of pronosupination only about 10 %, corresponding to an area of 1–2 mm, are in contact [95]; (b) *The inherent instability of the joint* necessitating the existence of different stabilizing mechanisms through intrinsic (intracapsular) as well as extrinsic (extracapsular) structures. The intrinsic

stability is provided by the dorsal and palmar radioulnar ligaments. Extrinsic stability is provided principally by the ECU tendon and sheath, the superficial and deep heads of the pronator quadratus and the interosseous ligament of the mid-forearm [90]. The distal interosseous ligament has variable thickness, ranging from 0.4 to 1.2 mm and when fully developed, constitutes the distal oblique band (DOB), which has a significant impact on DRUJ stability. Moritomo [125] in a recent anatomical study found that the DOB existed in 40 % of specimens and when present, it originates from the distal one-sixth of the ulnar shaft and runs distally to insert on the inferior rim of the sigmoid notch of the radius; (c) *The combined motion of rotation and translation* at the DRUJ, the articulating surfaces of which allow 150° of motion in pronation and supination of the forearm [87, 126, 127]. Bowers [128] and Pirela-Cruz [129] documented a mean palmar and dorsal translational motion of 2.2 mm, while the passive motion of the joint in a dorso–palmar direction causes a translational motion of 5.4 mm for palmar direction and 2.8 mm for dorsal direction. The translational motion is dorsal in pronation and palmar in supination [127], while according to Adams and Holley [130], the translation occurs mostly at the extremes of pronosupination.

In addition to the motions described, there also exists an abduction–adduction movement referred to, by Pirela-Cruz et al. [129], as diastatic motion. This motion occurs because of the cam-effect of the elliptical nature of the ulnar head as rotation takes place. Finally, one other motion of the DRUJ is the pistoning-type effect that is observed during rotation of the forearm and loading of the joint. Relative to the radius, the ulna moves distally with pronation and proximally with supination. With stress loading of the wrist the ulna moves distally relative to the radius [127].

The orientation of the articular surfaces of the ulnar head and the sigmoid notch is also of major clinical importance. Sagerman et al. [131] have radiographically shown that the inclination of these opposing articular surfaces is almost never parallel, and is usually much different. Relative to the long axis to the ulna, the ulnar seat inclination averages 21° (range, −13.8° to 40.5°), while the sigmoid notch inclination averages 7.7° (range, −24.3° to 26.8°). Consequences of this observation are: (a) The component of translation movement that accompanies the rotation of the forearm can be attributed, to some degree, to a difference in the degree of inclination, apart from the difference in the radii of curvature of the opposing articular surfaces; (b) Because of the wide variation between the inclination of the sigmoid notch and ulnar seat, symptomatic articular incongruity can occur following joint leveling procedures. Tolat [132] reports three basic configurations of the DRUJ, depending on the orientation of the articular surfaces: The vertical type (I) (38 %), the oblique type (II) (50 %), and the reverse type (III) (12 %) (Fig. 2.33a, b, c).

The role of the DRUJ capsule has been clarified by Kleinman and Graham [133]. They observed that the inferior capsule is strong and durable and may be involved in the stability of the joint. The volar and dorsal aspects of the capsule are compliant and accept the ulna head as the radiocarpal unit rotates and translates through the pronosupination arc. The contraction of this part of the capsule plays an important role in limiting the rotation of the forearm.

Ishii et al. [134] measured the pressure distribution within the DRUJ with axial loads applied to the wrist in varying degrees of forearm rotation. They found that: (a) by increasing application of an axial load across the wrist, the average area of the sigmoid notch in contact with the ulnar head also increased, and (b) In pronation, there is compressive loading between the dorsal sigmoid notch and the ulnar head; in supination there is compressive loading between the palmar sigmoid notch and the ulnar head. This was confirmed by Bowers [135] who claimed that on the extreme positions of pronation-supination, part of the stability of the joint can be attributed to the compression of the dorsal or volar rim of the sigmoid notch and the ulnar head.

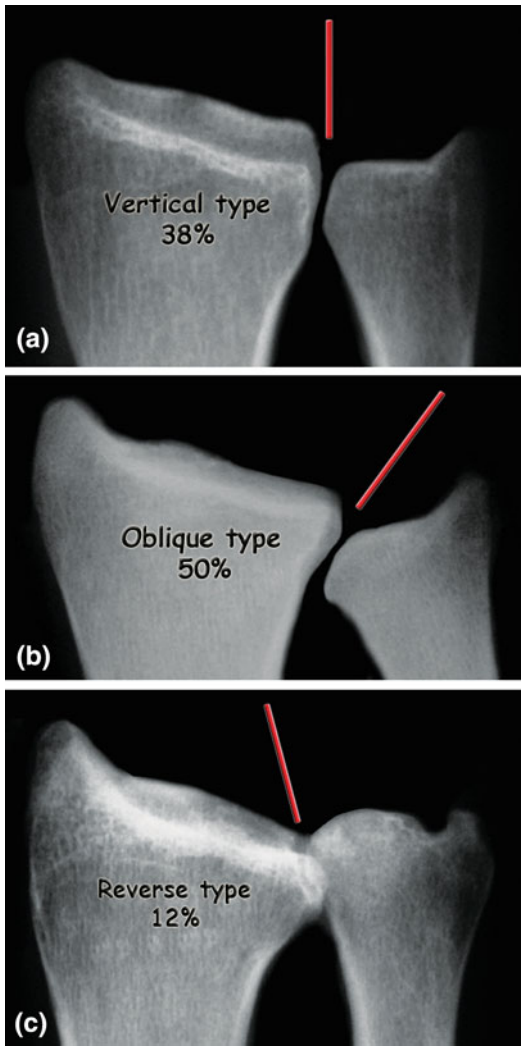

Fig. 2.33 The three basic configurations of the DRUJ depending on the orientation of the articular surfaces, according to Tolat [132] (**a**, **b**, **c**). With permission from [157]

2.3 Vascularity of the Wrist

The blood supply to the wrist is provided by an extrinsic and an intrinsic vascular system. The extrinsic blood supply is developed through branches of the radial, ulnar, and anterior interosseous arteries, which form an arcade of anastomosing branches that produce three dorsal and three palmar arches:

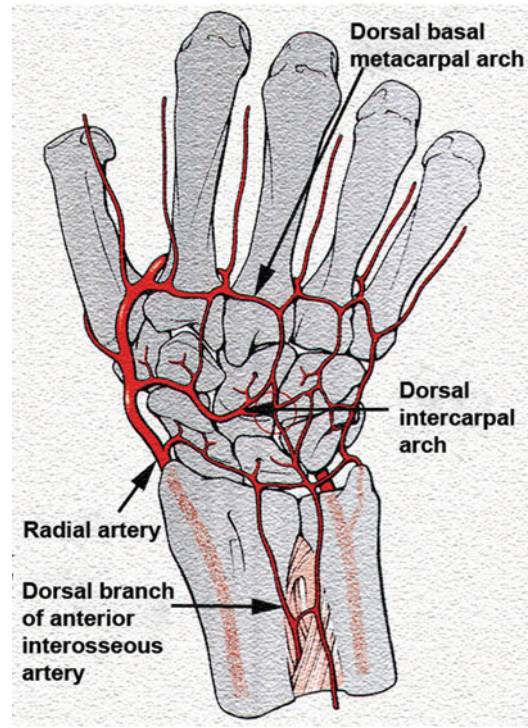

Fig. 2.34 Schematic drawing of the dorsal arterial network. With permission from [157]

(a) The dorsal and palmar radiocarpal arches;
(b) The dorsal and palmar intercarpal arches; and
(c) The dorsal basal metacarpal and the deep palmar arches (Figs. 2.34 and 2.35).

Gelberman et al. [136–138] found that on the dorsal surface, the largest and most consistent arch is the intercarpal arch, which provides the major blood supply to the distal carpal row and contributes to the vascularity of the lunate and the triquetrum. The next largest arch, the radiocarpal arch, was present in 75–80 % of the specimens. It supplies the distal radial metaphysic, as well as the lunate and the triquetrum from the dorsum. The basal metacarpal arch was often tenuous and was present in only 27 % of the specimens.

On the palmar surface, both the palmar radiocarpal arch and the deep palmar arch were present in 100 % of all specimens while the intercarpal arch was present in only 53 %. The

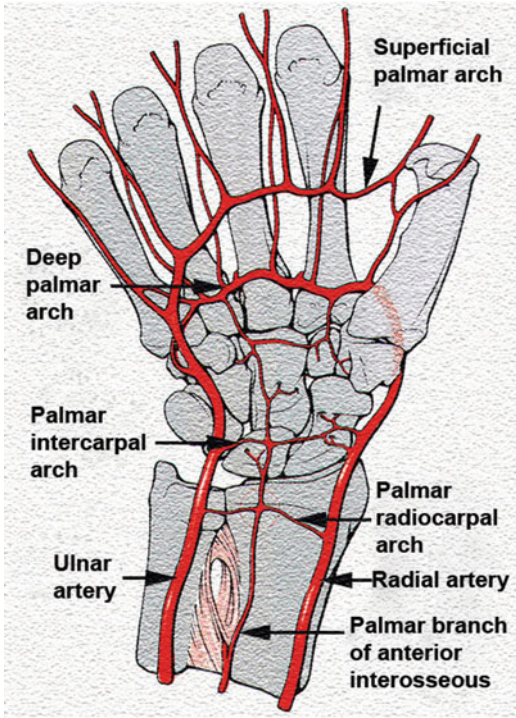

Fig. 2.35 Schematic drawing of the volar arterial network. With permission from [157]

palmar radiocarpal arch provides the major blood supply both to the lunate and to the triquetrum from the palmar surface. The deep palmar arch supplies the distal carpal row by way of radial and ulnar recurrent arteries (present in 100 %) and via the accessory ulnar recurrent artery (in 27 %). The intercarpal arch is small and inconsistent, and in no case does it make a significant contribution to the carpal bones.

The superficial palmar arch and the posterior interosseous artery do not appear to provide any substantial contribution to the vascular supply of the wrist. However, with their multiple vascular anastomoses, they provide significant collateral circulation to the wrist [136, 137].

The radial artery forms the lateral border and the ulnar artery forms the medial border of this system. The anterior interosseous artery has a palmar and dorsal division that form at the proximal border of the pronator quadrates. The dorsal division extends distally on the interosseous membrane to the carpus, where it joins the dorsal carpal arch that provides vascular supply to the proximal carpal row. The palmar division continues deep into the pronator quadrates and bifurcates into branches that communicate with the palmar radiocarpal arch supplying the lunate and the triquetrum, and finally enters the RSL ligament [139].

All but three carpal bones receive blood vessels directly from the dorsal and palmar arches: the scaphoid, pisiform, and trapezium have direct blood supply from the radial and ulnar arteries.

Panagis et al. [140] and Gelberman and Gross [137] classified the carpal bones into three groups on the basis of the number and location of nutrient vessels, the presence or absence of intraosseous anastomoses, and the dependence of large areas of bone on a single vessel. The clinical significance of the various groups is based on the risk of posttraumatic avascular necrosis for the bones in each group:

Group I (Scaphoid, Capitate, and 8 % [137] or 20 % [139] of the lunates). Includes carpal bones which either have vessels entering from only one surface, or large areas of bone that are dependent on a single vessel. This group is the most vulnerable to posttraumatic avascular necrosis.

Group II (Hamate, Trapezoid). Includes carpal bones, which have two or more areas of vessel entry but lack significant anastomoses within the entire or a major part of the bones. Specific injuries can compromise their blood supply.

Group III (Trapezium, triquetrum, pisiform, and 80 % [139] or 92 % [137] of the lunates). Includes carpal bones, which have two or more areas of vessel entry and consistent intraosseous anastomoses.

Vascularity of the scaphoid [136, 141]: The scaphoid receives its vascular supply mainly from the radial artery. Vessels enter dorsally and palmarly in the limited areas that are nonarticular of ligamentous attachment.

The *palmar vascular supply* is responsible for 20–30 % of the internal vascularity, all in the region of the distal pole. The palmar vascular supply is provided by: (a) the superficial palmar

branch, which at the level of the radioscaphoid joint is giving off the radial artery and (b) several smaller branches that are coursing distal to the origin of the superficial palmar branch to enter through the region of the tubercle. In 75 % of specimens, these arteries arise directly from the radial artery and in the remainder, they arise from the superficial palmar branch of the radial artery.

The *dorsal vascular supply* to the scaphoid accounts for 70–80 % of the internal vascularity of the bone, and supplies the waist and the proximal pole of the bone. The major dorsal vessels to the scaphoid enter the bone through small foramina located on the dorsal ridge. At the level of the intercarpal joint, the radial artery gives off the intercarpal artery, which participates in the formation of the dorsal intercarpal arch. Just proximal to the origin of the intercarpal artery, at the level of the styloid process of the radius, a vessel is given off to enter the scaphoid through its waist along the dorsal ridge. In 70 % of specimens, the dorsal vessel arises directly from the radial artery. In 23 %, the dorsal branch has its origin from the common stem of the intercarpal artery. In 7 %, the scaphoid receives its dorsal blood supply directly from the branches of the intercarpal artery and the radial artery. In all specimens, there are consistent major communications between the dorsal scaphoid branch of the radial artery and the dorsal branch of the anterior interosseous artery. It has been stated [38] that the vessels enter through the dorsal ridge in 79 %, distal to the waist in 14 %, and proximal to the waist in 7 % of specimens. The fact that in 14 % of specimens the blood supply enters distal to the waist means that approximately one out of seven specimens would have shown a significant loss of blood supply to the proximal pole following a fracture through the waist [2, 142].

Vascularity of capitate [139, 141]: The capitate receives its vascularity from dorsal and palmar sources. Most arteries enter the capitate distally and follow a retrograde proximal course to supply the rest of the bone. The main (dorsal) vascularity originates from vessels of the dorsal intercarpal and dorsal basal metacarpal arches. The palmar vascular supply arises from anastomosing branches of the recurrent ulnar artery, palmar radiocarpal arch, and deep palmar arch. In the majority of specimens (67 %) the dorsal vessels supply the major part of the capitate. In 33 % of specimens, the vascularity to the capitate head originates entirely from the palmar surface. There are notable anastomoses between the dorsal and the palmar blood supplies in 30 % of specimens. In the remainder there are no anastomoses seen.

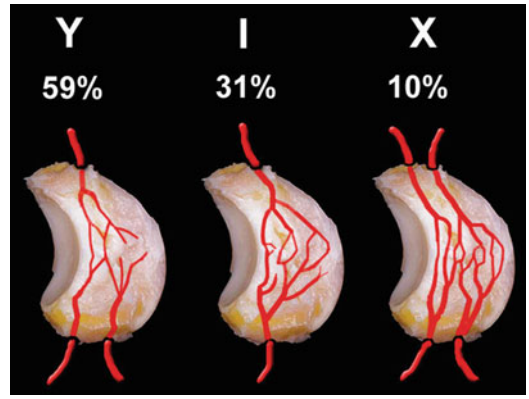

Fig. 2.36 Patterns of intraosseous vascularity of the lunate and the frequency of their appearance according to Gelberman et al. [143]. With permission from [157]

Vascularity of the lunate [141, 143]: The lunate receives its blood supply from both palmar and dorsal sources or from the palmar aspect alone. The vessels entering the dorsal surface are from branches of the dorsal radiocarpal arch, the dorsal intercarpal arch, and occasionally from smaller branches of the dorsal branch of the anterior interosseous artery. In 80 % of specimens, the lunate receives nutrient vessels from the palmar and dorsal surfaces. In 20 % of specimens, it receives nutrient vessels from the palmar surface alone. There are three major intraosseous patterns, which are formed in the shape of the letters Y, I, or X. (Fig. 2.36).

The Y pattern is the most common, occuring in 59 % of specimens studied. The stem of the Y occurs dorsally or palmarly, with equal frequency.

The I pattern occurs in 31 % of specimens, and consists of one dorsal and one palmar vessel that anastomose in a straight line.

The X pattern occurs in 10 % of specimens, consisting of two dorsal and two palmar vessels that anastomose in the center of the lunate.

Vascularity of the trapezoid [140]: The trapezoid is supplied by branches of the dorsal intercarpal, the basal metacarpal, and the radial recurrent artery. The nutrient vessels enter the trapezoid through its two nonarticular surfaces on the dorsal and palmar surfaces. Three or four small vessels enter the dorsal surface to supply the dorsal 70 % of the bone. These dorsal vessels provide the primary vascularity of the trapezoid. From the palmar surface one or two small vessels supply the palmar 30 % of the bone. The palmar vessels do not anastomose with the dorsal vessels.

Vascularity of the hamate [2, 141]: The vascularity of the hamate is supplied by the dorsal intercarpal arch, the ulnar recurrent artery of the deep palmar arch, and the ulnar artery. The vessels enter through the three nonarticular surfaces of the hamate, which include the dorsal, the palmar, and the medial surface through the hook of the hamate. The dorsal surface receives three to five vessels from the dorsal intercarpal arch which supply the dorsal 30–40 % of the bone. The palmar surface usually receives one large vessel that enters through the radial base of the hook. It then branches and anastomoses with the dorsal vessels in 50 % of the specimens studied. The hook of the hamate receives one or two small vessels that enter through the medial base and tip of the hook. These vessels anastomose with each other but usually not with the vessels to the body of the hamate.

Vascularity of the trapezium: The vascularity of the trapezium is by vessels from the distal branches of the radial artery. Nutrient vessels enter the trapezium through its three nonarticular surfaces: dorsal, radial, and palmar. Dorsally, the vascular supply predominates and one to three vessels enter and supply the entire dorsal aspect of the bone. Palmarly, one to three vessels enter and anastomose with the vessels entering through the dorsal surface. Radially, three to six small vessels penetrate the lateral surface and anastomose with the dorsal and palmar vessels.

Vascularity of the triquetrum: The triquetrum receives its blood supply from branches from the ulnar artery, the dorsal intercarpal arch, and the palmar intercarpal arch. Nutrient vessels enter through its two nonarticular surfaces on the dorsal and palmar aspects. Two to four vessels enter the dorsal ridge of the bone and supply the dorsal 60 % of the triquetrum. From the volar surface, one or two vessels enter proximal and distal to the facet that articulates with the pisiform and supply the palmar 40 % of the bone. The dorsal vessels provide the primary vascularity for the triquetrum in 60 % of the specimens while the palmar vessels constitute the main vascularity in 20 % of specimens. Significant anastomoses between the dorsal and palmar vascular networks have been found to be present in 86 % of specimens studied.

Vascularity of the pisiform: The pisiform receives one to three small vessels directly from the ulnar artery entering the bone at the proximal and distal poles. Vessels anastomose with each other just beneath the articular surface of the pisiform, assuming a vascular ring pattern that is consistently seen in all specimens.

2.4 Innervation of Wrist Ligaments

The innervation of the wrist joint capsule has been identified largely by reports associated with surgical denervation of the wrist for chronic pain [144–147].

The main innervation to the wrist capsule derives from the anterior interosseous nerve, lateral antebrachial cutaneous nerve, and posterior interosseous nerve. Other minor sources of capsular innervation include: The palmar cutaneous branch of the median nerve, the deep branch of the ulnar nerve, the superficial branch of the radial nerve, and the dorsal branch of the ulnar nerve [148].

The terminal branch of the *posterior interosseous nerve* innervates the dorsal capsules of the radiocarpal and midcarpal joints as well as the dorsal wrist ligaments. It also innervates the

dorsal capsules of the second, third, and fourth CMC joints [149]. It is considered to be the major dorsal source of innervation of the wrist. Minor contributions are also provided by the terminal branches of the dorsal sensory radial and ulnar nerves [71].

The terminal branch of the *anterior interosseous nerve* innervates the central two-thirds of the volar wrist capsule. Buck-Gramcko [149], however, defined this zone of innervation extending distally to include the palmar midcarpal joint and the central CMC joints.

The *lateral antebrachial cutaneous nerve* innervates the radial aspects of the radiocarpal and midcarpal joints and the first CMC joint [148, 150]. Other branches contributing less to the volar capsular innervation include the volar cutaneous branch of the median nerve and the deep branches from the ulnar nerve [71, 148].

The innervation to DRUJ and TFCC appears to be threefold, with the dorsal region (dorsal DRUJ capsule, DRU ligament, and dorsal ulnocarpal capsule) primarily innervated by branches of the posterior interosseous nerve, the ulnar region (MH, foveal attachment of the TFC, prestyloid recess, and UT ligament) primarily by articular extensions of the dorsal sensory branches of the ulnar nerve, and the volar region (volar DRUJ capsule, PRU ligament, and UL ligaments) by branches from the ulnar nerve [151, 152].

Recent investigations disputed the role of carpal ligaments as simple passive restraints. The microscopic innervation of the extrinsic and intrinsic wrist ligaments has been studied, to reveal a variable degree of sensory innervation by highly specialized nerve endings, called mechanoreceptors. The mechanoreceptors embedded into the ligaments, receive the mechanical signals and transform them into afferent nerve stimuli to influence periarticular muscles. In a recent study, Hagert et al. [153] made clear for the first time the existence of ligamento–muscular reflexes initiating in the carpal ligaments.

The innervation pattern of the wrist ligaments reflects in structural differences between the ligaments. Ligaments with limited innervation consisted mostly of densely packed collagen fibers. In the ligaments with abundant innervation, mechanoreceptors and nerve fascicles were consistently found in the loose connective tissue of the superficial region of the ligaments (epifascicular region), while the density of innervation was greatest close to the ligament insertions into bone [71]. Hagert et al. [154] found a pronounced innervation in the dorsal wrist ligaments (dorsal radiocarpal, dorsal intercarpal, scaphotriquetral, dorsal scapholunate interosseous), an intermediate innervation in the volar triquetral ligaments (palmar lunotriquetral interosseous, triquetrocapitate, triquetrohamate), and only limited/occasional innervation in the remaining volar wrist ligaments. They state that wrist ligaments are regarded as either mechanically or sensory important ligaments. The mechanically important ligaments are ligaments with densely packed collagen bundles, limited innervation, and are located primarily in the radial, force-bearing column of the wrist. The sensory important ligaments, by contrast, are richly innervated although less dense in connective tissue composition and are related to the triquetrum, which is the key element in the generation of the proprioceptive information.

Mataliotakis et al. [82] in a cadaver study investigated the sensory innervation of the subregions of the SLI ligament and found that the palmar subregion, apart from its major mechanical role, contains the greatest amount of neural structures and mechanoreceptors. The dorsal subregion, with densely packed collagen fibers and limited innervation, functions mainly to constrain the scaphoid-lunate relative motion.

Other studies evaluated the distribution of mechanoreceptors on the dorsal radiocarpal ligament [155], where the nerve endings predominate the superficial layer and the ligament insertions to the bone, or on the TFCC [156], where the nerve endings were distributed at the periphery of TFC and showed different concentrations of each type of mechanoreceptors per topographic area.

References

1. Berger RA (2001) The anatomy of the ligaments of the wrist and distal radioulnar joints. Clin Orthop 383:32–40
2. Taleisnik J (1985) The wrist. Churchill Livingstone, New York
3. Berger RA (2010) Wrist anatomy. In: Cooney W (ed) The wrist. Diagnosis and operative treatment, 2nd edn. Lippincott Williams & Wilkins, Philadelphia, pp 25–76
4. Berger RA (1997) The ligaments of the wrist: a current overview of anatomy with considerations of their potential functions. Hand Clin 13:63–82
5. Buijze GA, Lozano-Calderon SA, Strackee SD et al (2011) Osseous and ligamentous scaphoid anatomy: part I. A systematic literature review highlighting controversies. J Hand Surg [Am] 36:1926–1935
6. Buijze GA, Dvinskikh NA, Strackee SD et al (2011) Osseous and ligamentous scaphoid anatomy: part II. Evaluation of ligament morphology using three-dimensional anatomical imaging. J Hand Surg [Am] 36:1936–1943
7. Theumann NH, Pfirrmann CWA, Gregory AE et al (2003) Extrinsic carpal ligaments: normal MR arthrographic appearance in cadavers. Radiology 226:171–179
8. Sennwald S (1987) Anatomical approach: The wrist. Springer, Berlin, pp 13–46
9. Berger RA, Landsmeer JM (1990) The palmar radiocarpal ligaments: a study of adult and fetal human wrist joints. J Hand Surg [Am] 15:847–854
10. Ritt MJPF, Stuart PR, Berglund LJ et al (1995) Rotational stability of the carpus relative to the forearm. J Hand Surg [Am] 20:305–311
11. Katz DA, Green JK, Werner FW et al (2003) Capsuloligamentous restraints to dorsal and palmar carpal translation. J Hand Surg [Am] 28:610–613
12. Rayhack JM, Linscheid RL, Dobyns JH et al (1987) Posttraumatic ulnar translation of the carpus. J Hand Surg [Am] 12:180–189
13. Viegas SF, Patterson RM, Ward K (1995) Extrinsic wrist ligaments in the pathomechanics of ulnar translation instability. J Hand Surg [Am] 20:312–318
14. Watts AC, Mclean JM, Fogg Q et al (2011) Scaphoid anatomy. In: Slutsky DJ, Slade JF III (eds) The scaphoid. Thieme, New York, pp 3–10
15. Nowak MD (1991) Material properties of ligaments. In: An KN, Berger RA, Cooney WP (eds) Biomechanics of the wrist Joint. Springer, New York, pp 139–156
16. Siegel DB, Gelberman RH (1991) Radial styloidectomy: an anatomical study with special reference to radiocarpal intracapsular ligamentous morphology. J Hand Surg [Am] 16:40–44
17. Kwon BC, Choi SJ, Shin J et al (2009) Proximal row carpectomy with capsular interposition arthroplasty for advanced arthritis of the wrist. J Bone Joint Surg Br 91:1601–1606
18. Scobercea RG, Budoff JE, Hipp JA (2009) Biomechanical effect of triquetral and scaphoid excision on simulated midcarpal arthrodesis in cadavers. J Hand Surg [Am] 34:381–386
19. Moritomo H, Apergis E, Herzberg G et al (2011) Committee report on wrist biomechanics and instability: Carpal instability following scaphoid fracture. IFSSH Ezine 4: 14–17 Nov
20. Nagao S, Patterson RM, Buford WL et al (2005) Three-dimensional description of ligamentous attachments around the lunate. J Hand Surg [Am] 30:685–692
21. Kijima Y, Viegas S (2009) Wrist anatomy and biomechanics. J Hand Surg [Am] 34:1555–1563
22. Bogumill G (1988) Anatomy of the wrist. In: Lichtman D (ed) The wrist and its disorders. WB Saunders, Philadelphia, pp 14–26
23. Cardoso R, Szabo RM (2010) Wrist anatomy and surgical approaches. Hand Clin 26:1–19
24. Chee KG, Chin AYH, Chew EM, Garcia-Elias M (2012) Antipronation spiral tenodesis—a surgical technique for the treatment of perilunate instability. J Hand Surg [Am] 37:2611–2618
25. Berger RA, Blair WF (1984) The radioscapholunate ligament: a gross and histologic description. Anat Rec 210(2):393–405
26. Hixson ML (1990) Microvascular anatomy of the radioscapholunate ligament of the wrist. J Hand Surg [Am] 15:279–282
27. Cooney WP (1998) Arthroscopic anatomy of the wrist. In: Linscheid RL, Dobyns JH (eds) Cooney WP. The wrist. diagnosis and operative treatment. Mosby, Missouri, pp 169–187
28. Whipple TL (1995) The role of arthroscopy in the treatment of scapholunate instability. Hand Clin 11:37–40
29. Berger RA, Kauer JMG, Landsmeer JMF (1991) Radioscapholunate ligament: a gross anatomic and histologic study of fetal and adult wrists. J Hand Surg [Am] 16:350–355
30. Garcia-Elias M (1998) Soft-tissue anatomy and relationships about the distal ulna. Hand Clin 14(2):165–176
31. Wiesner L, Rumelhart C, Pham E et al (1996) Experimentally induced ulno-carpal instability. a study on 13 cadaver wrists. J Hand Surg [Br] 21(1): 24–29
32. Munk B, Jensen SL, Olsen BS et al (2005) Wrist stability after experimental traumatic triangular fibrocartilage complex lesions. J Hand Surg [Am] 30:43–49
33. Moritomo H, Murase T, Arimitsu S et al (2008) Change in the length of the ulnocarpal ligaments during radiocarpal motion: possible impact on triangular fibrocartilage complex foveal tears. J Hand Surg [Am] 33:1278–1286
34. Bos K (1996) Instability of the distal radioulnar joint. In: Büchler U (ed) Wrist instability. Martin Dunitz, London, pp 45–54

35. Ilyas AM, Mudgal CS (2008) Radiocarpal fracture-dislocations. J Am Acad Orthop Surg 16:647–655
36. Tay S-C, Berger RA, Parker WL (2010) Longitudinal split tears of the lunotriquetral ligament. Hand Clin 26:495–501
37. Moritomo H, Viegas SF, Nakamura K et al (2000) The scaphotrapezio-trapezoidal joint. Part 1: an anatomic and radiographic study. J Hand Surg [Am] 25:899–910
38. Boabighi A, Kuhlmann JN, Kenesi C (1993) The distal ligamentous complex of the scaphoid and the scapho-lunate ligament. An anatomic, histological and biomechanical study. J Hand Surg [Br] 18:65–69
39. Drewniany JJ, Palmer AK, Flatt AE (1985) The scaphotrapezial ligament complex: an anatomic and biomechanical study. J Hand Surg [Am] 10:492–498
40. Masquelet AC, Strube F, Nordin JY (1993) The isolated scapho-trapezio-trapezoid ligament injury. Diagnosis and surgical treatment in four cases. J Hand Surg [Br] 18:730–735
41. Kuo CE, Wolfe SW (2008) Scapholunate instability: current concepts in diagnosis and management. J Hand Surg [Am] 33:998–1013
42. Short WH, Werner FW, Green JK et al (2007) Biomechanical evaluation of the ligamentous stabilizers of the scaphoid and lunate: part III. J Hand Surg [Am] 32(3):297–309
43. Heras-Palou C (2009) Midcarpal instability. In: Slutsky DJ, Osterman AL (eds) Fractures and injuries of the distal radius and carpus. The cutting edge. Saunders, Philadelphia, pp 417–423
44. Moritomo H, Goto A, Sato Y et al (2003) The triquetrum-hamate joint: an anatomic and in vivo three-dimensional kinematic study. J Hand Surg [Am] 28:797–805
45. Moritomo H, Murase T, Goto A et al (2004) Capitate-based kinematics of the midcarpal joint during wrist radioulnar deviation: an in vivo three-dimensional motion analysis. J Hand Surg [Am] 29(4):668–675
46. Moritomo H, Apergis E, Herzberg G et al (2007) 2007 IFSSH Committee report of wrist biomechanics committee: Biomechanics of the so-called dart-throwing motion of the wrist. J Hand Surg [Am] 32:1447–1453
47. Garcia-Elias M (2008) The non-dissociative clunking wrist: a personal view. J Hand Surg [Eur] 33(6):698–711
48. Andermahr J, Lozano-Calderon S, Trafton T et al (2006) The volar extension of the lunate facet of the distal radius: a quantitative anatomic study. J Hand Surg [Am] 31:892–895
49. Nakamura K, Patterson RM, Moritomo H et al (2001) Type I versus type II lunates: ligament anatomy and presence of arthrosis. J Hand Surg [Am] 26:428–436
50. Sennwald GR, Zdravkovic V, Oberlin C (1994) The anatomy of the palmar scaphotriquetral ligament. J Bone Joint Surg Br 76:147–149
51. Sennwald G, Zdravkovic V, Fischer M (1996) Wrist arthroscopy: can you see instability? In: Büchler U (ed) Wrist instability. Martin Dunitz, London, pp 56–60
52. Viegas SF, Yamaguchi S, Boyd NL et al (1999) The dorsal ligaments of the wrist: anatomy, mechanical properties, and function. J Hand Surg [Am] 24:456–468
53. Viegas SF (2001) The dorsal ligaments of the wrist. Hand Clin 17(1):65–75
54. Berger RA, Garcia-Elias M (1991) General anatomy of the wrist. In: Kai-Nan A, Berger RA, Cooney WP III (eds) Biomechanics of the wrist joint. Springer, Berlin, pp 1–22
55. Shaaban H, Lees VC (2006) The two parts of the dorsal radiocarpal (radiolunotriquetral) ligament. J Hand Surg [Br] 31(2):13–215
56. Mizuseki T, Ikuta Y (1989) The dorsal carpal ligaments: their anatomy and function. J Hand Surg [Br] 14:91–98
57. Smith DK (1993) Dorsal carpal ligaments of the wrist: normal appearance on multiplanar reconstructions of three-dimensional fourier transform MR imaging. Am J Roentgen 161:119–125
58. Short WH, Werner FW, Green JK et al (2002) The effect of sectioning the dorsal radiocarpal ligament and insertion of a pressure sensor into the radiocarpal joint on scaphoid and lunate kinematics. J Hand Surg [Am] 27:68–76
59. Viegas SF, Patterson RM, Peterson PD et al (1990) Ulnar-sided perilunate instability: an anatomic and biomechanic study. J Hand Surg [Am] 15:268–278
60. Horii E, Garcia-Elias M, An KN et al (1991) A kinematic study of luno-triquetral dissociations. J Hand Surg [Am] 16:355–362
61. Nanno M, Patterson RM, Viegas SF (2006) Three-dimensional imaging of the carpal ligaments. Hand Clin 22:399–412
62. Sokolow C, Saffar P (2001) Anatomy and histology of the scapholunate ligament. Hand Clin 17:77–81
63. Moritomo H, Murase T, Oka K et al (2008) Relationship between the fracture location and the kinematic pattern in scaphoid nonunion. J Hand Surg [Am] 33:1459–1468
64. Moritomo H, Viegas SF, Elder KW et al (2000) Scaphoid nonunions: a 3-dimensional analysis of patterns of deformity. J Hand Surg [Am] 25:520–528
65. Slater RR, Szabo RM (1999) Scapholunate dissociation: treatment with the dorsal intercarpal ligament capsulodesis. Techn Hand Upper Extrem Surg 3:222–228
66. Slater RR, Szabo RM, Bay BK et al (1999) Dorsal intercarpal ligament capsulodesis for scapholunate dissociation: biomechanical analysis in a cadaver model. J Hand Surg [Am] 24:232–239
67. Walsh JJ, Berger RA, Cooney WP (2002) Current status of scapholunate interosseous ligament injuries. J Am Acad Orthop Surg 10:32–42

68. Mitsuyasu H, Patterson RM, Shah MA et al (2004) The role of the dorsal intercarpal ligament in dynamic and static scapholunate instability. J Hand Surg [Am] 29:279–288
69. Viegas SF, Dasilva MF (2000) Surgical repair for scapholunate dissociation. Techn Hand Upper Extrem Surg 4:148–153
70. Berger RA, Bishop AT, Bettinger PC (1995) New dorsal capsulotomy for the surgical exposure of the wrist. Ann Plast Surg 35:54–59
71. Hagert E, Ferreres A, Garcia-Elias M (2010) Nerve-sparing dorsal and volar approaches to the radiocarpal joint. J Hand Surg [Am] 35:1070–1074
72. Gelberman RH, Cooney WP, Szabo RM (2000) Carpal instability. J Bone Joint Surg Am 82:578–594
73. Ritt MJPF, Bishop AT, Berger RA et al (1998) Lunotriquetral ligament properties: a comparison of three anatomic subregions. J Hand Surg [Am] 23:425–431
74. Berger RA, Imeada T, Berglund L et al (1999) Constraint and material properties of the subregions of the scapholunate interosseous ligament. J Hand Surg [Am] 24:953–962
75. Ruby LK, An K-N, Linscheid RL et al (1987) The effect of scapholunate ligament section on scapholunate motion. J Hand Surg [Am] 12:767–771
76. Short WH, Werner FW, Fortino MD et al (1995) A dynamic biomechanical study of scapholunate ligament sectioning. J Hand Surg [Am] 20:986–999
77. Conyers DJ (1990) Scapholunate interosseous reconstruction and imbrication of palmar ligaments. J Hand Surg [Am] 15:690–700
78. Marcuzzi A, Acciaro AL, Caserta G et al (2006) Ligamentous reconstruction of scapholunate dislocation through a double dorsal and palmar approach. J Hand Surg [Br] 31(4):445–449
79. Dunn MJ, Johnson C (2001) Static scapholunate dissociation: a new reconstruction technique using a volar and dorsal approach in a cadaver model. J Hand Surg [Am] 26:749–754
80. Berger RA, Blair WF, Crowninshield RD et al (1982) The scapholunate ligament. J Hand Surg [Am] 7(1):87–91
81. Nikolopoulos F, Apergis E, Poulilios A et al (2011) Biomechanical properties of the scapholunate ligament and the importance of its portions in the capitate intrusion injury. Clin Biomech 26:819–823
82. Mataliotakis G, Doukas M, Kostas I et al (2009) Sensory innervation of the subregions of the scapholunate interosseous ligament in relation to their structural composition. J Hand Surg [Am] 34:1413–1421
83. Ritt MJPF, Berger RA, Bishop AT et al (1996) The capitohamate ligaments. J Hand Surg [Br] 21(4):451–454
84. Garcia-Elias M, An KN, Cooney WP III et al (1989) Stability of the transverse carpal arch: an experimental study. J Hand Surg [Am] 14:277–282
85. Palmer AK, Werner FW (1981) The triangular fibrocartilage complex of the wrist-anatomy and function. J Hand Surg [Am] 6:153–162
86. Palmer AK, Glisson RR, Werner FW (1984) Relationship between ulnar variance and triangular fibrocartilage complex thickness. J Hand Surg [Am] 9:681–682
87. Chidgey LK (1995) The distal radioulnar joint: problems and solutions. J Am Acad Orthop Surg 3:95–109
88. Nakamura T, Takayama S, Horiuchi Y et al (2001) Origins and insertions of the triangular fibrocartilage complex: a histological study. J Hand Surg [Br] 26(5):446–454
89. Gabl M, Zimmermann R, Angermann P et al (1998) The interosseous membrane and its influence on the distal radioulnar joint. An anatomical investigation of the distal tract. J Hand Surg [Br] 23:179–182
90. Kleinmann W (2007) Stability of the distal radioulnar joint: biomechanics, pathophysiology, physical diagnosis, and restoration of function. What we have learned in 25 Years. J Hand Surg [Am] 32(7):1086–1106
91. Ishii S, Palmer AK, Werner FW et al (1998) An anatomic study of the ligamentous structure of the triangular fibrocartilage complex. J Hand Surg [Am] 23:977–985
92. Af Ekenstam F, Hagert CG (1985) Anatomical studies on the geometry and stability of the distal radio ulnar joint. Scand J Plast Reconstr Surg 19:17–25
93. Schuind F, An KN, Berglund L et al (1991) The distal radioulnar ligaments: a biomechanical study. J Hand Surg [Am] 16:1106–1114
94. Hagert CG (1994) Distal radius fracture and the distal radioulnar joint—anatomical considerations. Handchir Mikrochir Plast Chir 26:22–26
95. Hagert E, Hagert CG (2010) Understanding stability of the distal radioulnar joint through an understanding of its anatomy. Hand Clin 26:459–466
96. Mikic ZD (1978) Age changes in the triangular fibrocartilage of the wrist joint. J Anat 126:367–384
97. Nakamura T, Yabe Y, Horiuch IY (1996) Functional anatomy of the triangular fibrocartilage complex. J Hand Surg [Br] 21(5):581–586
98. Thiru-Pathi RG, Ferlic DC, Clayton ML et al (1986) Arterial anatomy of the triangular fibrocartilage of the wrist and its surgical significance. J Hand Surg [Am] 11:258–263
99. Bednar MS, Arnoczky SP, Weiland AJ (1991) The microvasculature of the triangular fibrocartilage complex: Its clinical significance. J Hand Surg [Am] 16:1101–1105
100. Burgess RC (1990) Anatomic variations of the midcarpal joint. J Hand Surg [Am] 15:129–131
101. Canovas F, Roussanne Y, Captier G et al (2004) Study of carpal bone morphology and position in three dimensions by image analysis from computed tomography scans of the wrist. Surg Radiol Anat 26(3):186–190

102. Viegas SF (2001) Advances in the skeletal anatomy of the wrist. Hand Clin 17(1):1–11
103. Moojen TM, Snel JG, Venema HW et al (2003) In Vivo analysis of carpal kinematics and comparative review of the literature. J Hand Surg [Am] 28:81–87
104. Craigen MAC, Stanley JK (1995) Wrist kinematics. Row, column or both? J Hand Surg [Br] 20(2):165–170
105. Garcia-Elias M, Ribe M, Rodriguez J et al (1995) Influence of joint laxity on scaphoid kinematics. J Hand Surg [Br] 20(3):379–382
106. Compson JP, Waterman JK, Heatley FW (1994) The radiological anatomy of the scaphoid. Part 1: osteology. J Hand Surg [Br] 19:183–187
107. Ceri N, Korman E, Gunal I et al (2004) The morphological and morphometric features of the scaphoid. J Hand Surg [Br] 29(4):393–398
108. Heinzelmann AD, Archer G, Bindra RR (2007) Anthropometry of the human scaphoid. J Hand Surg [Am] 32:1005–1008
109. Moojen TM, Snel JG, Ritt MJPF et al (2002) Scaphoid kinematics in vivo. J Hand Surg [Am] 27:1003–1010
110. Moritomo H, Viegas S, Elder K et al (2000) The scaphotrapezio-trapezoidal joint. Part 2: a kinematic study. J Hand Surg [Am] 25:911–920
111. Wolfe SW, Neu C, Crisco J (2000) In vivo scaphoid, lunate, and capitate kinematics in flexion and in extension. J Hand Surg [Am] 25:860–869
112. Berger RA (2001) The anatomy of the scaphoid. Hand Clin 17:525–532
113. Fogg Q (2004) Scaphoid variation and an anatomical basis for variable carpal mechanics. Department of Anatomical Sciences, University of Adelaide. Thesis
114. Garcia-Elias M, Lluch AL, Stanley JK (2006) Three-ligament tenodesis for the treatment of scapholunate dissociation: Indications and surgical technique. J Hand Surg [Am] 31:125–134
115. Short WH, Werner FW, Green JK et al (2005) Biomechanical evaluation of the ligamentous stabilizers of the scaphoid and lunate: Part II. J Hand Surg [Am] 30:24–34
116. Wolfe SW (2001) Scapholunate instability. J Am Soc Surg Hand 1(1):45–60
117. Schuind FA, Linscheid RL, An K-N et al (1992) A normal data base of posteroanterior roentgenographic measurements of the wrist. J Bone Joint Surg Am 74(9):1418–1429
118. Werner FW, Short WH, Green JK et al (2007) Severity of scapholunate instability is related to joint anatomy and congruency. J Hand Surg [Am] 32:55–60
119. Mclean JM, Turner PC, Bain GI et al (2009) An association between lunate morphology and scaphoid–trapezium–trapezoid arthritis. J Hand Surg [Eur] 34(6):778–782
120. Viegas SF, Wagner K, Patterson R et al (1990) Medial (hamate) facet of the lunate. J Hand Surg [Am] 15:564–571
121. Nakamura K, Beppu M, Patterson RM et al (2000) Motion analysis in two dimensions of radial–ulnar deviation of type I versus type II lunates. J Hand Surg [Am] 25:877–888
122. Haase SC, Berger RA, Shin AY (2007) Association between lunate morphology and carpal collapse patterns in scaphoid nonunions. J Hand Surg [Am] 32:1009–1012
123. Nakamura K, Beppu M, Matsushita K et al (1997) Biomechanical analysis of the stress force on midcarpal joint in Kienbock's disease. Hand Surg 2:101–115
124. Mclean J, Bain G, Eames M et al (2006) An anatomic study of the triquetrum– hamate joint. J Hand Surg [Am] 31:601–607
125. Moritomo H (2012) The distal interosseous membrane: current concepts in wrist anatomy and biomechanics. J Hand Surg [Am] 33(7):1501–1507
126. Imbriglia JE, Clifford JW (2001) Management of the painful distal radioulnar joint. Lippincott Williams & Wilkins, Philadelphia
127. Loftus JB, Palmer AK (1997) Disorders of the distal radioulnar joint and triangular fibrocartilage complex: an overview. In: Lichtman DM, Alexander AH (eds) The wrist and its disorders, 2nd edn. WB Saunders Co, Philadelphia, pp 385–414
128. Bowers WH (1993) The distal radial ulnar joint. In: Green DP (ed) Operative hand surgery, 3rd edn. Churchill Livingstone, Philadelphia, pp 973–1019
129. Pirela-Cruz MA (1991) Stress computed tomography analysis of the distal radioulnar joint: a diagnostic tool for determining translational motion. J Hand Surg [Am] 16:75–81
130. Adams BD, Holley KA (1993) Strains in the articular disk of the triangular fibrocartilage complex: a biomechanical study. J Hand Surg [Am] 18:919–925
131. Sagerman SD, Zogby RG, Palmer AK et al (1995) Relative articular inclination of the distal radioulnar joint: a radiographic study. J Hand Surg [Am] 20:597–601
132. Tolat AR (1992) The gymnast's wrist: acquired positive ulnar variance following chronic epiphyseal injury. J Hand Surg [Br] 17:678–681
133. Kleinman WB, Graham TJ (1998) The distal radioulnar joint capsule: clinical anatomy and role in posttraumatic limitation of forearm rotation. J Hand Surg [Am] 23:588–599
134. Ishii S, Palmer AK, Werner FW et al (1996) Pressure distribution in the distal radioulnar joint. In: Presented at the 51st annual meeting of the American society for surgery of the hand nashville, TN
135. Bowers WH (1991) Instability of the distal radioulnar articulation. Hand Clin 7:311–328
136. Gelberman RH, Menon J (1980) The vascularity of the scaphoid bone. J Hand Surg [Am] 5(5):508–513

137. Gelberman RH, Gross MS (1986) The vascularity of the wrist. Identification of arterial patterns at risk. Clin Orthop 202:40–49
138. Gelberman RH, Botte MJ (1997) Vascularity of the carpus. In: Lichtman DM, Alexander AH (eds) The wrist and its disorders. WB Saunders Co, Philadelphia, pp 34–47
139. Cooney WP (1998) Vascular and neurologic anatomy of the wrist. In: Cooney WP, Linscheid RL, Dobyns JH (eds) The wrist. Diagnosis and operative treatment. Mosby, Missouri, pp 106–123
140. Panagis JS, Gelberman RH, Taleisnik J (1983) The arterial anatomy of the human carpus. Part II: the intraosseous vascularity. J Hand Surg [Am] 8:375–382
141. Freedman DM, Botte MJ, Gelberman RH (2001) Vascularity of the carpus. Clin Orthop 383:47–59
142. Schmidt H-M, Lanz U (2004) Surgical anatomy of the Hand. Georg Thieme Verlag, New York
143. Gelberman RH, Bauman TD, Menon J et al (1980) The vascularity of the lunate bone and Kienbock's disease. J Hand Surg [Am] 5(3):272–278
144. Braga-Silva J, Román JA, Padoin AV (2011) Wrist denervation for painful conditions of the wrist. J Hand Surg [Am] 36:961–966
145. Ferreres A, Foucher G, Suso S (2002) Extensive denervation of the wrist. Techn Hand Upper Extrem Surg 6(1):36–41
146. Grechenig W, Mahring M, Clement HG (1998) Denervation of the radiocarpal joint. J Bone Joint Surg Br 80:504–507
147. Wilhelm A (1965) Denervation of the wrist [in German]. Hefte Unfallheilkd 81:109–114
148. Van de Pol GJ, Koudstaal MJ, Schuurman AH et al (2006) Innervation of the wrist joint and surgical perspectives of denervation. J Hand Surg [Am] 31:28–34
149. Buck-Gramcko D (1977) Denervation of the wrist joint. J Hand Surg [Am] 2:54–61
150. Fukumoto K, Kojima T, Kinoshita Y et al (1993) An anatomic study of the innervation of the wrist joint and Wilhelm's technique for denervation. J Hand Surg [Am] 18(3):484–489
151. Gupta R, Nelson SD, Baker J et al (2001) The innervation of the triangular fibrocartilage complex: nitric acid maceration rediscovered. Plast Reconstr Surg 107(1):135–139
152. Shigemitsu T, Tobe M, Mizutani K et al (2007) Innervation of the triangular fibrocartilage complex of the human wrist: quantitative immunohistochemical study. Anat Sci Int 82(3): 127–132
153. Hagert E, Persson JKE, Werner M et al (2009) Evidence of wrist proprioceptive reflexes elicited after stimulation of the scapholunate interosseous ligament. J Hand Surg [Am] 34:642–651
154. Hagert E, Garcia-Elias M, Forsgren S et al (2007) Immunohistochemical analysis of wrist ligament innervation in relation to their structural composition. J Hand Surg [Am] 32:30–36
155. Tomita K, Berger EJ, Berger RA et al (2007) Distribution of nerve endings in the human dorsal radiocarpal ligament. J Hand Surg [Am] 32:466–473
156. Cavalcante MLC, Rodrigues CJ, Rames M (2004) Mechanoreceptors and nerve endings of the triangular fibrocartilage in the human wrist. J Hand Surg [Am] 29:432–435
157. Apergis E (2004) *καταγματα-εξαρθρήματα του καρπου*. Konstantaras Medical Books, Athens